










RESEARCH ARTICLE

Loss of G0/G1 switch gene 2 (GOS2) promotes disease progression and drug resistance in chronic myeloid leukaemia (CML) by disrupting glycerophospholipid metabolism

Mayra A. Gonzalez¹  | Idaly M. Olivas^{1,2}  | Alfonso E. Bencomo-Alvarez¹  |
Andres J. Rubio^{1,3} | Christian Barreto-Vargas⁴  | Jose L. Lopez³ | Sara K. Dang^{2,3} |
Jonathan P. Solecki² | Emily McCall³ | Gonzalo Astudillo³ | Vanessa V. Velazquez³ |
Katherine Schenkel³ | Kelaiah Reffell² | Mariah Perkins³ | Nhu Nguyen³ |
Jehu N. Apaflo⁵ | Efren Alvidrez⁶ | James E. Young² | Joshua J. Lara^{2,3} |
Dongqing Yan⁷ | Anna Senina⁷ | Jonathan Ahmann⁷ | Katherine E. Varley⁷  |
Clinton C. Mason⁷ | Christopher A. Eide⁸ | Brian J. Druker⁸  | Md Nurunnabi⁶  |
Osvaldo Padilla⁹ | Sudip Bajpeyi⁵  | Anna M. Eiring^{1,2,3} 

¹Department of Molecular and Translational Medicine, Center of Emphasis in Cancer, Texas Tech University Health Sciences Center El Paso, El Paso, Texas, USA

²L. Frederick Francis Graduate School of Biomedical Sciences, Texas Tech University Health Sciences Center El Paso, El Paso, Texas, USA

³Paul L. Foster School of Medicine, Texas Tech University Health Sciences Center El Paso, El Paso, Texas, USA

⁴Immunology Division, University of Guadalajara, Guadalajara, Jalisco, Mexico

⁵Metabolic, Nutrition and Exercise Research (MiNER) Laboratory, Department of Kinesiology, University of Texas at El Paso, El Paso, Texas, USA

⁶Department of Pharmaceutical Sciences, School of Pharmacy, University of Texas at El Paso, El Paso, Texas, USA

⁷Huntsman Cancer Institute, The University of Utah, Salt Lake City, Utah, USA

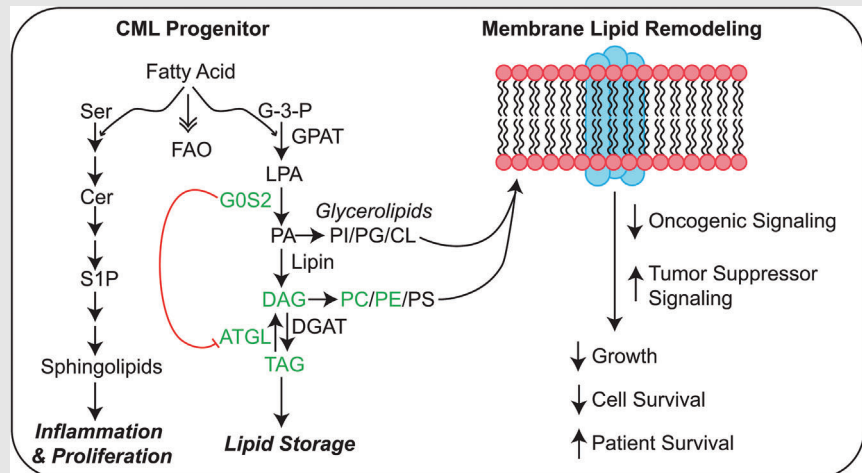
⁸Knight Cancer Institute, Division of Hematology/Medical Oncology, Oregon Health & Science University, Portland, Oregon, USA

⁹Department of Pathology, Texas Tech University Health Sciences Center El Paso, El Paso, Texas, USA

Correspondence

Anna M. Eiring, 5001 El Paso Drive, MSC
32002, MSB1 Room 2112, El Paso, TX 79905,
USA.










Email: anna.eiring@ttuhsc.edu

Graphical Abstract

1. GOS2 is reduced in disease progression and drug resistance of CML.
2. GOS2 expression impairs survival of CML progenitors with little effect on apoptosis.
3. GOS2 function in CML is independent of its known function as an inhibitor of adipose triglyceride lipase (ATGL), the rate-limiting enzyme for intracellular lipolysis.
4. Loss of GOS2 disrupts glycerophospholipid metabolism in CML and promotes therapy resistance.

RESEARCH ARTICLE

Loss of G0/G1 switch gene 2 (GOS2) promotes disease progression and drug resistance in chronic myeloid leukaemia (CML) by disrupting glycerophospholipid metabolism

Mayra A. Gonzalez¹  | Idaly M. Olivas^{1,2}  | Alfonso E. Bencomo-Alvarez¹  |
Andres J. Rubio^{1,3} | Christian Barreto-Vargas⁴  | Jose L. Lopez³ | Sara K. Dang^{2,3} |
Jonathan P. Solecki² | Emily McCall³ | Gonzalo Astudillo³ | Vanessa V. Velazquez³ |
Katherine Schenkel³ | Kelaiah Reffell² | Mariah Perkins³ | Nhu Nguyen³ |
Jehu N. Apaflo⁵ | Efren Alvidrez⁶ | James E. Young² | Joshua J. Lara^{2,3} |
Dongqing Yan⁷ | Anna Senina⁷ | Jonathan Ahmann⁷ | Katherine E. Varley⁷  |
Clinton C. Mason⁷ | Christopher A. Eide⁸ | Brian J. Druker⁸  | Md Nurunnabi⁶  |
Osvaldo Padilla⁹ | Sudip Bajpeyi⁵  | Anna M. Eiring^{1,2,3} 

¹Department of Molecular and Translational Medicine, Center of Emphasis in Cancer, Texas Tech University Health Sciences Center El Paso, El Paso, Texas, USA

²L. Frederick Francis Graduate School of Biomedical Sciences, Texas Tech University Health Sciences Center El Paso, El Paso, Texas, USA

³Paul L. Foster School of Medicine, Texas Tech University Health Sciences Center El Paso, El Paso, Texas, USA

⁴Immunology Division, University of Guadalajara, Guadalajara, Jalisco, Mexico

⁵Metabolic, Nutrition and Exercise Research (MiNER) Laboratory, Department of Kinesiology, University of Texas at El Paso, El Paso, Texas, USA

⁶Department of Pharmaceutical Sciences, School of Pharmacy, University of Texas at El Paso, El Paso, Texas, USA

⁷Huntsman Cancer Institute, The University of Utah, Salt Lake City, Utah, USA

⁸Knight Cancer Institute, Division of Hematology/Medical Oncology, Oregon Health & Science University, Portland, Oregon, USA

⁹Department of Pathology, Texas Tech University Health Sciences Center El Paso, El Paso, Texas, USA

Correspondence

Anna M. Eiring, 5001 El Paso Drive, MSC
32002, MSB1 Room 2112, El Paso, TX
79905, USA.
Email: anna.eiring@ttuhsc.edu

Funding information

National Cancer Institute of the National
Institutes of Health, Grant/Award
Numbers: K22CA216008, R01CA065823;
Seed Grant Funding to Catalyse
UTEP-TTUHSC El Paso Joint Research
Funding Projects

Abstract

Tyrosine kinase inhibitors (TKIs) targeting BCR::ABL1 have turned chronic myeloid leukaemia (CML) from a fatal disease into a manageable condition for most patients. Despite improved survival, targeting drug-resistant leukaemia stem cells (LSCs) remains a challenge for curative CML therapy. Aberrant lipid metabolism can have a large impact on membrane dynamics, cell survival and therapeutic responses in cancer. While ceramide and sphingolipid levels were previously correlated with TKI response in CML, the role of lipid metabolism

This is an open access article under the terms of the [Creative Commons Attribution](https://creativecommons.org/licenses/by/4.0/) License, which permits use, distribution and reproduction in any medium, provided the original work is properly cited.

© 2022 The Authors. *Clinical and Translational Medicine* published by John Wiley & Sons Australia, Ltd on behalf of Shanghai Institute of Clinical Bioinformatics.

in TKI resistance is not well understood. We have identified downregulation of a critical regulator of lipid metabolism, G0/G1 switch gene 2 (*G0S2*), in multiple scenarios of TKI resistance, including (1) BCR::ABL1 kinase-independent TKI resistance, (2) progression of CML from the chronic to the blast phase of the disease, and (3) in CML versus normal myeloid progenitors. Accordingly, CML patients with low *G0S2* expression levels had a worse overall survival. *G0S2* downregulation in CML was not a result of promoter hypermethylation or BCR::ABL1 kinase activity, but was rather due to transcriptional repression by MYC. Using CML cell lines, patient samples and *G0s2* knockout (*G0s2*^{-/-}) mice, we demonstrate a tumour suppressor role for *G0S2* in CML and TKI resistance. Our data suggest that reduced *G0S2* protein expression in CML disrupts glycerophospholipid metabolism, correlating with a block of differentiation that renders CML cells resistant to therapy. Altogether, our data unravel a new role for *G0S2* in regulating myeloid differentiation and TKI response in CML, and suggest that restoring *G0S2* may have clinical utility.

KEYWORDS

chronic myeloid leukaemia (CML), G0/G1 switch gene 2 (*G0S2*), glycerophospholipid metabolism, tyrosine kinase inhibitor (TKI) resistance

1 | INTRODUCTION

Chronic myeloid leukaemia (CML) is caused by BCR::ABL1, a constitutively active fusion tyrosine kinase.¹ A majority of CML patients present in the chronic phase (CP-CML), where ABL1 tyrosine kinase inhibitors (TKIs) have revolutionised disease therapy, turning it from a lethal disease into a manageable condition for most patients. Despite the success, 10%–15% of patients fail first-line TKI therapy,² necessitating treatment changes to limit the risk of progression to the rapidly fatal blast phase of CML (BP-CML), characterised by differentiation blockade and therapy resistance.^{3,4} Additionally, TKIs do not eliminate the residual CML leukaemic stem cell (LSC) population,^{5,6} with disease recurrence common after TKI discontinuation.^{7–9} Thus, new therapeutic combination strategies are required to overcome persistent CML LSCs to minimise the risk of progression and improve rates and durability of treatment-free remission.

Half of clinical TKI resistance is free of BCR::ABL1 kinase domain mutations,¹⁰ suggesting BCR::ABL1 kinase-independent resistance mechanisms, the primary form of TKI resistance in CML LSCs.¹¹ From a previously reported gene expression classifier study that predicted a patient's response to first-line imatinib, mRNA encoding G0/G1 switch gene 2 (*G0S2*) was identified among the most downregulated genes in TKI resistance.¹² *G0S2* is a small protein that regulates multiple cellular

functions, including apoptosis,¹³ quiescence,^{14,15} lipolysis,^{16–18} de novo lipogenesis¹⁹ and oxidative phosphorylation (OxPhos).^{20–22} Additionally, *G0S2* is an all-trans retinoic acid (ATRA) target gene in acute promyelocytic leukaemia (APL).^{18,23,24} In the K562 CML cell line and normal haematopoietic stem cells (HSCs), *G0S2* inhibits proliferation by direct interaction with nucleolin^{14,15}; however, its role in CML blastic transformation and TKI resistance remains unknown. We hypothesised that *G0S2* plays a tumour suppressor role in CML, and that downregulation of *G0S2* contributes to reduced responses to TKI therapy. Altogether, our findings suggest that loss of *G0S2* occurs in multiple contexts of TKI resistance and progression in CML, and that restoring *G0S2* expression in such scenarios may have clinical utility by promoting myeloid differentiation and restoring TKI sensitivity.

2 | MATERIALS AND METHODS

2.1 | Cell lines and patient samples

Details regarding the culture of cell lines and primary cells are available in Supporting Information. Mononuclear cells (MNCs) from cord blood (CB) or peripheral blood (PB) of CML patients (see Table S1) were separated by density centrifugation on Ficoll-Paque PREMIUM

(GE Healthcare Systems, Chicago, IL, USA). CD34⁺ cells were selected using an autoMACS system (Miltenyi Biotec, San Diego, CA, USA) or the EasySep Human CD34 Positive Selection Kit II (Stem Cell Technologies, Vancouver, British Columbia, Canada). Samples were confirmed to have >90% purity by flow cytometry on a BD FAC-SCanto (BD Biosciences, San Jose, CA, USA). All CML cells were confirmed to harbour native *BCR::ABL1* as previously described (see Table S1).²⁵ Patient samples that did not have a *BCR::ABL1* kinase domain mutation were specifically selected for use in this study, and all BP-CML specimens were confirmed to be exclusively myeloid in nature. Fresh or frozen CD34⁺ cells from CML patients or normal CB were cultured in Iscove's Modified Dulbecco's Medium (IMDM, Life Technologies, Carlsbad, CA, USA) supplemented with 10% BIT9500 (Stem Cell Technologies), 100 U/ml penicillin–streptomycin (Life Technologies), 2 mM L-glutamine (Life Technologies) and recombinant cytokines (CC100; Stem Cell Technologies) or human granulocyte-colony stimulating factor (hG-CSF, 25 ng/ml, 7–10 days) (PeproTech, Inc., Cranbury, NJ, USA). Where indicated, cells were treated with the *BCR::ABL1* TKI, imatinib (1 μ M, Selleck Chemicals, Houston, TX, USA) or the *MYC* proto-oncogene (*MYC*) inhibitors, MYCi361 or MYCi975 (6 μ M, Selleck Chemicals). All patients gave informed consent in accordance with the Declaration of Helsinki, and all studies were approved by the Institutional Review Boards (IRBs) at the University of Utah, Texas Tech University Health Sciences Center El Paso and Oregon Health & Science University.

2.2 | Reverse transcription-quantitative polymerase chain reaction

RNA extraction was performed using the RNeasy Mini Kit (Qiagen, Hilden, Germany) and converted to cDNA with the iScript cDNA Synthesis Kit (Bio-Rad, Hercules, CA, USA). Human *GOS2*, *ATGL*, *BCR::ABL1* and *GUSB* levels were measured by reverse transcription-quantitative polymerase chain reaction (RT-qPCR) using the SsoAdvanced SYBR Green Supermix (Bio-Rad) in a CFX96 Real-Time PCR Detection System (Bio-Rad). Murine *G0s2* and *Gapdh* levels were measured using the Luna Universal One-Step qPCR Kit (New England Biolabs, Ipswich, MA, USA) on a StepOnePlus Real-Time PCR System (Applied Biosystems, Foster City, CA, USA). Primers are listed in Table S2. Assays were performed in triplicate, and relative expression was analysed using the comparative cycle threshold method ($2^{-\Delta\Delta C_t}$).

2.3 | Immunoblot

CML cell lines and primary CD34⁺ cells were cultured under the indicated conditions (24–72 h). Following drug or cytokine exposure, cells were lysed (4°C; 30 min) in Radio-Immunoprecipitation Assay (RIPA) buffer (Cell Signaling Technology, Danvers, MA, USA) containing protease (Complete Mini, Roche, Basel, Switzerland) and phosphatase (PhosStop, Roche) inhibitors. Samples were denatured (100°C; 10 min) prior to SDS-PAGE and transferred to polyvinylidene difluoride (PVDF) membranes. Antibodies are listed in Table S3. Densitometry was conducted using ImageJ (National Institutes of Health, Bethesda, MD, USA).

2.4 | Plasmids, virus packaging and infection

shRNAs targeting human *GOS2* (shG0S2), murine *G0s2* (shG0s2) or human *ATGL* (shATGL) were purchased from Celecta (Mountain View, CA, USA, Table S4). Constructs contain the wild-type tetracycline repressor, and vector expression requires culture with 0.1 μ g/ml doxycycline (72 h). For ectopic expression, *GOS2* was PCR amplified from MNCs of a healthy donor and subcloned into the indicated vectors (see Supporting Information). pCDH-puro-cMyc was a gift from Jialiang Wang (Addgene #46970).²⁶ MSCV-*BCR::ABL1*-IRES-GFP was a kind gift from Michael Deininger.^{27,28} Lentivirus-producing 293FT cells (Thermo Fisher Scientific, Waltham, MA, USA) were cultured in Dulbecco's Modified Eagle Medium (DMEM, Life Technologies) plus 10% fetal bovine serum (FBS, Thermo Fisher Scientific), 2.0 mM L-glutamine (Thermo Fisher Scientific), 1.0 mM sodium pyruvate (Life Technologies), 0.1 mM Minimum Essential Medium (MEM) non-essential amino acids (Life Technologies) and 100 U/ml penicillin–streptomycin (Life Technologies). Retrovirus-producing 293T/17 cells were purchased from American Type Culture Collection (Manassas, VA, USA) and cultured in 10% FBS, 2.0 mM L-glutamine and 100 U/ml penicillin–streptomycin. Lentiviral constructs were packaged in combination with vesicular stomatitis virus glycoprotein (VSV-G) (Clontech Laboratories, Inc., Mountain View, CA, USA) and psPax2 (Celecta), and concentrated 100 \times using polyethylene glycol 8000 (Thermo Fisher Scientific). Retrovirus constructs were packaged in combination with VSV-G and pCL-Eco (Addgene), and crude retroviral supernatants were used for transduction of cells in vitro. Viral vectors are listed in Table S4. We transfected virus-producing cells using the ProFection Mammalian

Transfection System (Promega, Madison, WI, USA). Derivative lines were generated by spinoculation of viral particles into cells, followed by fluorescence-activated cell sorting (FACS) of green fluorescent protein-positive (GFP⁺) cells or selection in puromycin (2 µg/ml, 72 h).

2.5 | Clonogenic assays

Methylcellulose clonogenic assays were performed by plating cells (10³) in 0.9% MethoCult (Stem Cell Technologies). Primary CD34⁺ cells were cultured with cytokines (CC100, Stem Cell Technologies) in the presence or absence of 1 µM imatinib and/or the indicated cytokines added directly to the medium. Cells were incubated in humid chambers at 37°C ± 0.1 µg/ml doxycycline in duplicate. Colonies were scored after 1–2 weeks in culture.

2.6 | Flow cytometry

To detect apoptosis, APC-AnnexinV (BD Biosciences) was used with 7-aminoactinomycin D (eBioscience, San Diego, CA, USA). To assess *G0S2* expression in stem versus progenitor cells, CD34⁺ cells from CB or CP-CML patients were sorted by FACS for HSCs, multipotent progenitors (MPPs), common myeloid progenitors (CMPs), granulocyte–macrophage progenitors (GMPs) and megakaryocyte–erythrocyte progenitors (MEPs)²⁹ (see Supporting Information and Table S3).

2.7 | DNA bisulphite conversion and patch PCR sequencing

DNA bisulphite conversion and patch PCR sequencing were performed on DNA from CD34⁺ cells from normal CB or CP-CML, BP-CML or TKI-resistant CML patients.³⁰ Sequencing reads were aligned to the reference genome (hg19) using Bismark software.³¹ For additional details, see Supporting Information.

2.8 | Chromatin immunoprecipitation

TKI-sensitive K562^S or TKI-resistant K562^R cells (2 × 10⁶) were crosslinked using 18% formaldehyde for 10 min at 37°C followed by quenching with 1.25 M glycine for 5 min at room temperature. Nuclear extracts were subjected to chromatin immunoprecipitation (ChIP) as outlined in Supporting Information.

2.9 | Animal models

Lineage-negative bone marrow (BM) cells from 6-week-old wild-type or *G0s2*^{-/-} mice³² were selected using the EasySep Mouse Hematopoietic Progenitor Cell Isolation Kit (Stem Cell Technologies). Resulting lineage-negative cells were cultured in recombinant murine kit ligand (10 ng/ml), interleukin (IL)-3 (2 ng/ml), IL-6 (1.2 ng/ml), Flt3 ligand (5 ng/ml) and granulocyte-macrophage-colony stimulating factor (GM-CSF, 5 ng/ml) (PeproTech), and either cultured ± murine G-CSF (mG-CSF, 25 ng/ml, 7–10 days) in in vitro differentiation assays or transduced with the MSCV-BCR::ABL1-IRES-GFP vector. In the latter experiment, 3 × 10⁵ unsorted GFP^{-/+} cells were injected intravenously into lethally irradiated (2 × 450 Rad, RS 2000, Rad Source Technologies, Inc., Buford, GA, USA) recipient mice. *BCR::ABL1* expression was confirmed in the peripheral blood of recipient mice by RT-qPCR. GFP⁺ cells in the BM of moribund recipient mice were quantified by flow cytometry on a BD FACSCanto (BD Biosciences). Haematoxylin and eosin staining of recipient spleens (4 weeks post-injection, *n* = 3 mice/group) was performed at the University of Texas Health Sciences Center San Antonio Department of Pathology and Laboratory Medicine (San Antonio, TX, USA). Complete blood counts were obtained using a HemaVet 950 haematology analyser (Drew Scientific, Miami Lakes, FL, USA). All experiments were approved by the Institutional Animal Care and Use Committee at Texas Tech University Health Sciences Center El Paso. See Supporting Information for details on subcutaneous injections.

2.10 | Gene expression analyses

Cell line RNA sequencing (RNAseq) is described in Supporting Information (GSE171945). Gene-level expression data for *G0S2* were obtained from primary CML patient MNCs isolated from either peripheral blood or BM and subjected to paired-end 2 × 150 bp RNAseq using the Illumina HiSeq platform.³³ Samples were obtained following informed consent in association with Oregon Health & Science University IRB protocol #4422. Patient samples were separated by disease phase or TKI response: CP-CML (*n* = 53), accelerated phase CML (AP-CML, *n* = 12), BP-CML (*n* = 13), newly diagnosed CP-CML (*n* = 21) and TKI-resistant CML (*n* = 42). All TKI-resistant CML patient samples had BCR::ABL1 kinase-independent resistance, defined by loss of a molecular and/or cytogenetic response to one or more TKIs without the presence of an explanatory BCR::ABL1 kinase domain mutation.³³ Gene expression

analyses using publicly available data are described in Supporting Information.

2.11 | Lipid profiling

Cells were cultured \pm doxycycline (0.1 $\mu\text{g}/\text{ml}$, 72 h) to induce *GOS2* ectopic expression or knockdown. Altered *GOS2* expression was confirmed at the mRNA and protein levels prior to analyses. Liquid chromatography (LC)/mass spectrometry (MS)-based lipidomics experiments were performed at Creative Proteomics (Shirley, NY, USA). For LC/MS-based lipidomics analyses, lipids were isolated using chloroform:MeOH (2:1) and centrifuged for 10 min at 3000 rpm at 4°C. The lower phase was transferred to a new tube for evaporation and dried under liquid nitrogen. Dried extracts were suspended in 200 μl isopropanol:MeOH (1:1) for internal standard analysis. Separation was performed by ultra-performance liquid chromatography (Thermo, Ultimate 3000LC). The LC system was comprised of a Phenomenex Kinetex C18 (100 mm \times 2.1 mm, 1.7 μm) column. The flow rate of the mobile phase was 0.3 ml/min. The column temperature was maintained at 40°C, and the sample manager temperature was set at 4°C. The raw data were acquired and aligned using the LipidSearchTM software (Thermo) based on the *m/z* value and the retention time of the ion signals. Ions from either ESI⁻ or ESI⁺ were merged and imported into the SIMCA-P software program version v.14.1 (Umetrics, Umea, Sweden) for multivariate analysis. A principal components analysis (PCA) was first used as an unsupervised method for data visualisation and outlier identification. Supervised regression modelling was then performed on the dataset by use of partial least squares discriminant analysis (PLS-DA) or orthogonal partial least squares discriminant analysis (OPLS-DA) to identify the potential lipid biomarkers. The biomarkers were filtered and confirmed by combining the results of the VIP values (VIP > 1.5) with a fold change (FC) of >2. To investigate the latent relationships of the lipids, we constructed a correlation network diagram based on Kyoto Encyclopedia of Genes and Genomes (KEGG) databases. All significant lipids were imported to obtain the categorical lipid annotations. Pathway enrichment analysis of the lipids dysregulated by *GOS2* ectopic expression or knockdown was performed using Lipid Pathway Enrichment Analysis (<https://lpea.biotec.tu-dresden.de/home>, Biomedical Cybernetics Group, Dresden, Germany).

2.12 | Statistical analyses

All experiments were performed in triplicate unless otherwise noted. Correlation of *GOS2* mRNA levels with survival

in CML was established using survival data available for 35 patients from the McWeeney et al. microarray.¹² CEL files from the original study¹² were imported with Partek software (Partek Inc., St. Louis, MO, USA) followed by GeneChip-Robust Multiarray Averaging (GC-RMA) normalisation. Expression levels were calculated from the microarray (HG-U133A, Affymetrix, Inc., Santa Clara, CA, USA) and dichotomised into high and low groups based on data distribution. Overall survival was assessed with Kaplan–Meier curves generated in Prism v6.04 (GraphPad Software Inc., San Diego, CA, USA). Statistical analyses were performed in SAS v9.3 (SAS Institute, Cary, NC, USA), and *p*-values are two-sided from a log-rank test. A two-tailed Student's *t*-test was used for cell line, mouse and patient sample data demonstrating equivocal variance; the Wilcoxon–Mann–Whitney test was used for unequivocal data.³⁴ Paired data were assessed with the Wilcoxon signed-rank test. Statistical analyses were performed using Microsoft Excel 2013 (Redmond, WA, USA) or Prism v7 (GraphPad Software Inc.).

3 | RESULTS

3.1 | *GOS2* is downregulated in CML disease progression and imatinib resistance in a BCR::ABL1 kinase-independent manner

A gene expression classifier was reported to predict a patient's imatinib response after 12 months of therapy.¹² *GOS2* mRNA was substantially downregulated in both imatinib non-responders who lack kinase domain mutations (GSE14671, Figure S1A),^{12,35} and in BP-CML versus CP-CML patients in another study (E-MEXP-480, Figure S1B).³⁶ An independent dataset comparing CD34⁺ cells from normal versus CP-CML patient BM showed consistent results (GDS2342, Figure S1C).³⁷ In contrast, there was no difference in *GOS2* expression comparing CD34⁺ BM cells from healthy volunteers with that of CP-CML patients who reached major molecular remission during imatinib therapy (GDS838, Figure S1D).³⁸ We further confirmed *GOS2* downregulation in CML by RT-qPCR analyses. These data demonstrated a 3.8-fold reduction of *GOS2* expression in CD34⁺ cells from newly diagnosed CP-CML patients compared with normal CB, with further downregulation by 3.1-fold in myeloid BP-CML (Figure 1A). While CML patients with kinase-independent TKI resistance had reduced *GOS2* expression compared with normal CB, there was no significant difference compared with CP-CML or BP-CML patients (Figure 1A). Immunoblotting confirmed the downregulation of *GOS2* protein in CD34⁺ cells from CML patients compared with

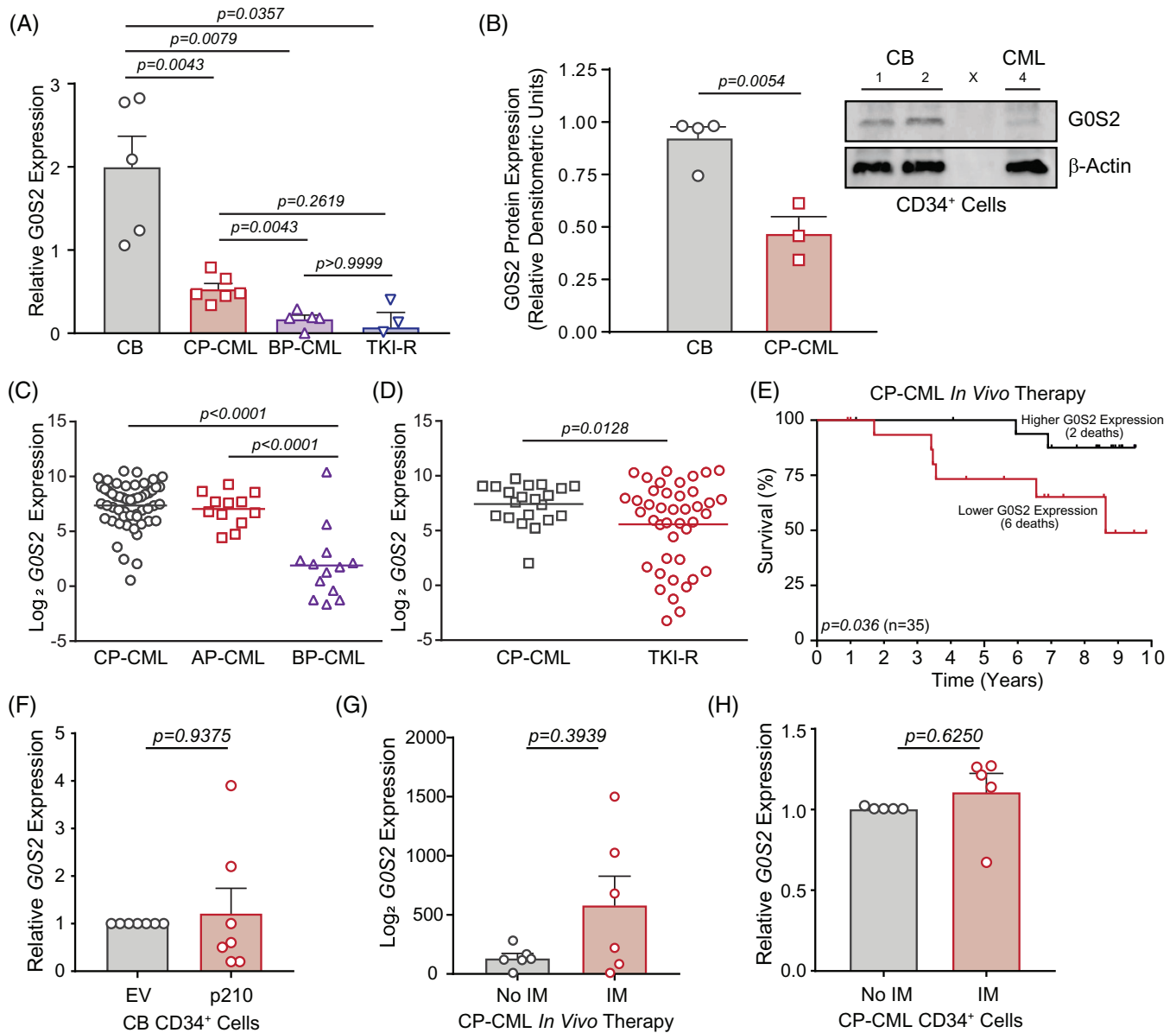


FIGURE 1 G0/G1 switch gene 2 (*G0S2*) is downregulated in chronic myeloid leukaemia (CML) disease progression and imatinib resistance in a BCR::ABL1 kinase-independent manner. (A) Bar graph shows *G0S2* mRNA levels as quantified by reverse transcription-quantitative polymerase chain reaction (RT-qPCR) on primary CD34⁺ cells from human cord blood (CB) ($n = 5$), chronic phase CML (CP-CML) ($n = 6$), blast phase CML (BP-CML) ($n = 5$) and tyrosine kinase inhibitor-resistant (TKI-R) patients harbouring native BCR::ABL1 ($n = 3$). (B) *G0S2* protein levels were analysed by immunoblot on primary CD34⁺ cells from human CB ($n = 4$) versus CP-CML patients ($n = 3$). β -Actin was analysed as a loading control. Bar graph represents relative densitometric units for primary cell immunoblot data. (C and D) Dot plots from RNAseq data demonstrate reduced *G0S2* mRNA levels in mononuclear cells from BP-CML ($n = 13$) compared with CP-CML ($n = 53$) and accelerated phase CML (AP-CML) ($n = 12$) patients (C), and in TKI-resistant ($n = 42$) compared with newly diagnosed ($n = 21$) CP-CML patients (D). (E) Kaplan-Meier curve shows relative overall survival (OS) of newly diagnosed CP-CML patients ($n = 35$) with *G0S2* mRNA expression in CD34⁺ cells (prior to imatinib therapy) above (high, $n = 18$) or below (low, $n = 17$) the value at a bimodal separation. (F) Bar graph shows relative *G0S2* mRNA levels in CB CD34⁺ cells engineered for p210 BCR::ABL1 ectopic expression ($n = 7$) versus the empty vector (EV) control ($n = 7$). (G) Bar graph demonstrates published microarray data showing *G0S2* mRNA expression levels in CP-CML CD34⁺ cells before and after *in vivo* imatinib (IM) therapy (400 mg daily) for 7 days ($n = 6$) (<https://www.ncbi.nlm.nih.gov/geo/profiles>, GDS3518, 213524_s_at, $p = .3939$).³⁹ (H) Bar graph shows *G0S2* mRNA expression in primary CP-CML CD34⁺ cells ($n = 5$) cultured *ex vivo* \pm IM (1 μ M, 24 h) as assessed by RT-qPCR. *GUS* mRNA levels were used as a loading control. Error bars represent standard error of the mean (SEM).

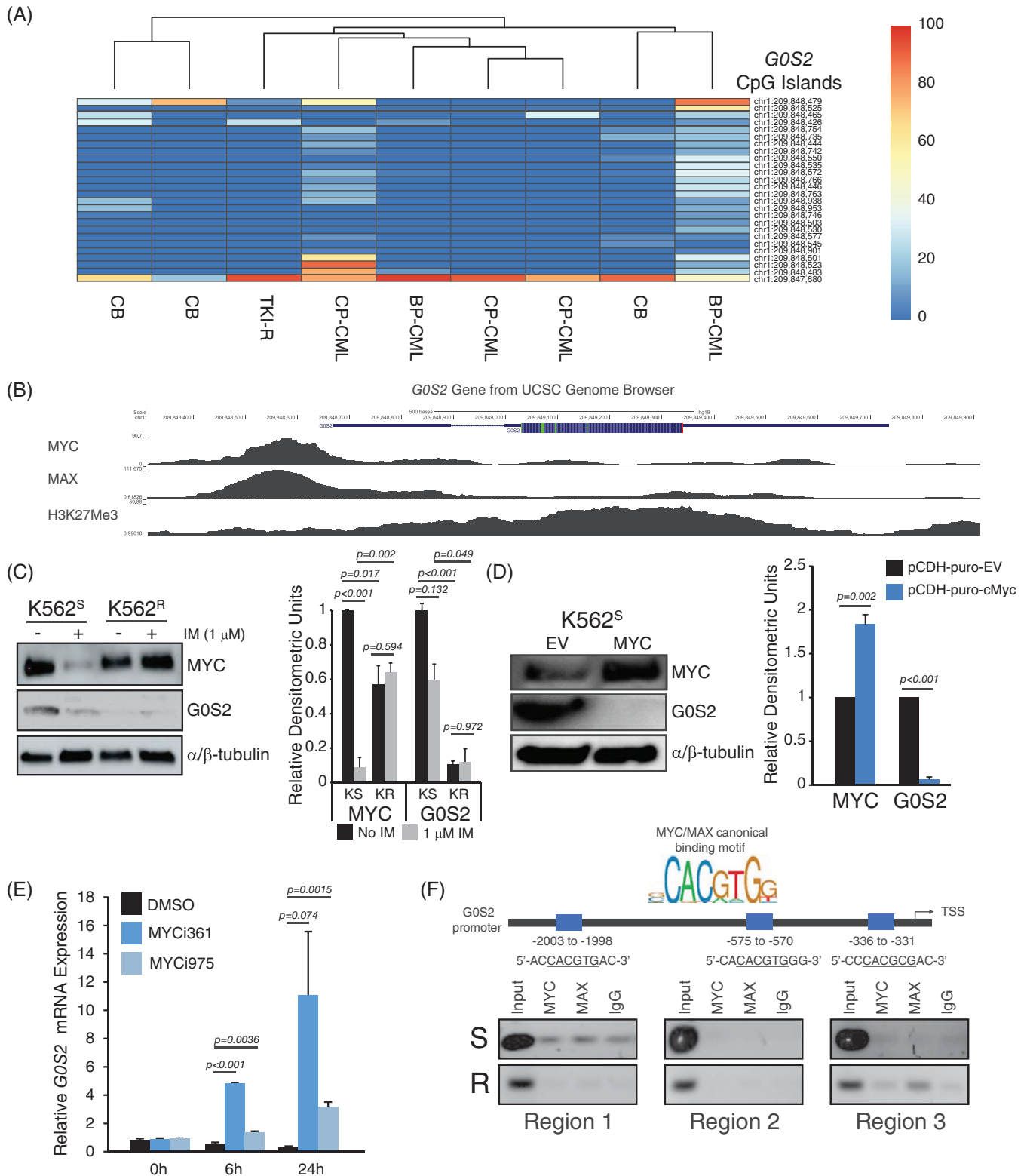


FIGURE 2 MYC/MAX mediates transcriptional repression of G0/G1 switch gene 2 (*G0S2*) in tyrosine kinase inhibitor-resistant (TKI-R) chronic myeloid leukaemia (CML). (A) The heat map represents CpG dinucleotide methylation in the *G0S2* promoter region as detected by DNA bisulphite conversion and patch polymerase chain reaction (PCR) sequencing on DNA of CD34⁺ cells from cord blood (CB) ($n = 3$) and CML patients ($n = 6$). (B) Tracks from the University of California at Santa Cruz Genome Browser (<https://genome.ucsc.edu/>) show a high degree of binding by MYC and MAX at the human *G0S2* promoter in K562 cells. (C) Immunoblot shows elevated MYC and decreased G0S2 protein expression in TKI-R K562^R cells compared with TKI-sensitive K562^S controls in the presence of imatinib (IM, 1 μM, 24 h). α/β -Tubulin was assessed as a loading control. Bar graph represents relative densitometric units for $n = 3$ replicates of the experiment. (D) Immunoblot and bar graph showing MYC and G0S2 protein expression in K562^S cells transfected with EV or MYC. The bar graph represents relative densitometric units for MYC and G0S2, comparing pCDH-puro-EV (black) and pCDH-puro-cMyc (blue) constructs. (E) Bar graph showing relative *G0S2* mRNA expression in K562 cells treated with DMSO, MYC361, or MYC1975 at 0h, 6h, and 24h. The bar graph represents relative *G0S2* mRNA expression for $n = 3$ replicates of the experiment. (F) Schematic of the *G0S2* promoter region and ChIP analysis. The schematic shows the promoter region from -2003 to -1998, -575 to -570, and -336 to -331 bp upstream of the TSS. The MYC/MAX canonical binding motif (CACGTGG) is highlighted. ChIP analysis was performed in K562 cells transfected with MYC or MAX, followed by immunoprecipitation (IP) with anti-MYC or anti-MAX antibodies. Input DNA and immunoprecipitated DNA were analyzed by immunoblotting for MYC and MAX in three regions (Region 1, Region 2, Region 3).

normal CB (Figure 1B). RNAseq data on an independent patient cohort showed reduced *GOS2* expression in patients with myeloid BP-CML and kinase-independent TKI resistance (Figure 1C,D). Finally, lower *GOS2* expression in CD34⁺ cells from a TKI-naïve CP-CML cohort was associated with worse overall survival (Figure 1E). Collectively, *GOS2* is downregulated in CML disease progression and TKI resistance, which correlates with worse outcomes.

We hypothesised that loss of *GOS2* in CML was a direct effect of BCR::ABL1 kinase activity. Surprisingly, forced expression of p210^{BCR::ABL1} in normal CB CD34⁺ cells resulted in no significant change in *GOS2* mRNA expression (Figure 1F). *GOS2* mRNA expression was unchanged in CML patients following 7 days of in vivo imatinib therapy (GDS3518, Figure 1G)³⁹ or when CML CD34⁺ cells were cultured ex vivo in the presence of imatinib (Figure 1H). Altogether, these data suggest that *GOS2* downregulation in CML and TKI resistance is independent of BCR::ABL1 kinase activity.

3.2 | MYC/MAX mediates transcriptional repression of *GOS2* in CML

The *GOS2* promoter is methylated and silenced in multiple different cancers,^{40–42} including the K562 CML cell line.⁴³ Consistently, treatment of BP-CML cell lines and primary cells with the DNA methyltransferase inhibitor, 5-azacytidine, increased *GOS2* mRNA expression (Figure S2). However, DNA bisulphite conversion and patch PCR sequencing³⁰ revealed no CpG dinucleotide methylation near the *GOS2* promoter in primary CD34⁺ cells (Figure 2A), suggesting alternative mechanisms for *GOS2* downregulation in CML. ENCODE ChIP-sequencing datasets (University of California, Santa Cruz Genome Browser) demonstrated that MYC/MAX occupies a region upstream of the *GOS2* transcription start site (TSS, Figure 2B). MYC is a nuclear phosphoprotein that regulates a variety of cellular functions, including cell growth, cell cycle, apoptosis and lipid metabolism.^{44,45} MYC also plays a role in CML disease progression, LSC survival and TKI resistance.^{46,47} We previously generated TKI-resistant K562 cells (K562^R) that are adapted for growth in the continuous presence of 1 μM imatinib and harbour native BCR::ABL1.⁴⁸ MYC expression was upregulated in TKI-resistant K562^R versus parental K562^S

cells in the presence of imatinib, which correlated with reduced *GOS2* protein expression (Figure 2C). These data suggest that MYC expression is BCR::ABL1-dependent in TKI-sensitive cells, but BCR::ABL1-independent in TKI-resistant cells. We hypothesised that MYC binds the *GOS2* promoter to repress its transcription, as previously reported for other genes.⁴⁹ Consistently, ectopic expression of MYC in parental K562 cells rapidly reduced *GOS2* protein expression (Figure 2D), whereas MYC inhibition led to rapid upregulation of *GOS2* mRNA in K562 cells (Figure 2E). To determine whether this effect was direct or indirect, we mapped MYC binding sites within the *GOS2* promoter, and performed ChIP using anti-MYC and anti-MAX antibodies compared with an IgG control in K562^R versus K562^S cells. MYC/MAX was enriched in region 3 upstream of the *GOS2* TSS (Figure 2F). These data indicate that upregulation of MYC is at least in part responsible for reduced *GOS2* expression in CML disease progression and TKI resistance.

3.3 | *GOS2* expression impairs survival without affecting apoptosis in CML

To determine whether *GOS2* is mechanistically involved in TKI resistance or strictly a biomarker, we lentivirally transduced CML cell lines and patient samples for *GOS2* ectopic expression using two separate vectors, and confirmed *GOS2* upregulation by immunoblot analyses and/or RT-qPCR (Figure S3A,B). Ectopic *GOS2* expression significantly reduced colony formation of both parental K562^S and TKI-resistant K562^R cells ± imatinib (Figure S3C). Importantly, the effect of ectopic *GOS2* was significantly greater in K562^R versus K562^S cells ($p = .022$). Conversely, we obtained three separate shRNA vectors targeting *GOS2* (sh*GOS2*), and confirmed knockdown at the mRNA and protein levels (Figure S3D,E). Knockdown of *GOS2* significantly increased clonogenic capacity of K562^S cells in both the absence and presence of graded doses of imatinib (Figure S3F). In primary cells, ectopic *GOS2* expression impaired colony formation in CP-CML and BP-CML CD34⁺ cells cultured ex vivo ± imatinib (Figure 3A,B, left). Again, the effects of ectopic *GOS2* were significantly greater in BP-CML compared with CP-CML ($p = .006$). Although *GOS2* was reported to promote apoptosis by binding to and antagonising BCL2,¹³ ectopic *GOS2* had no effect on

shows the level of MYC and *GOS2* protein in K562^S cells engineered for MYC overexpression. α/β -Tubulin was assessed as a loading control. Bar graph represents the relative densitometric units for $n = 3$ replicates of the experiment. (E) Bar graph shows relative *GOS2* mRNA expression in K562 cells treated with the MYC inhibitors, MYCi361 or MYCi975 (6 μM) for 0, 6 and 24 h. (F) MYC consensus binding sites were mapped onto the *GOS2* promoter, and the presence of MYC or MAX at the relevant site was detected by chromatin immunoprecipitation (ChIP)-PCR ($n = 3$). Error bars represent standard error of the mean (SEM). BP-CML, blast phase CML; CP-CML, chronic phase CML; EV, empty vector

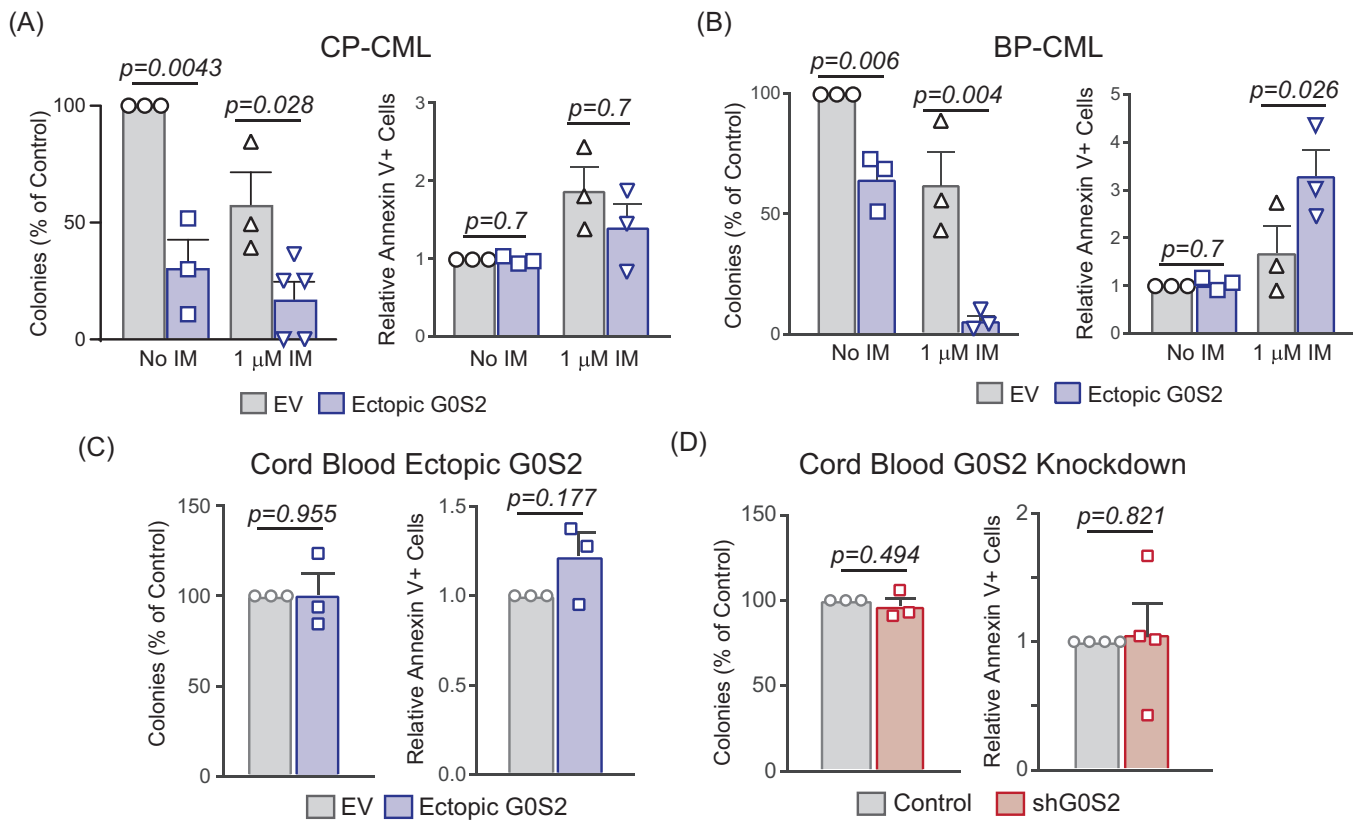


FIGURE 3 G0/G1 switch gene 2 (G0S2) acts as a tumour suppressor in primary chronic myeloid leukaemia (CML) CD34⁺ cells by impairing survival without affecting apoptosis. (A and B) Primary CD34⁺ cells isolated from chronic phase CML (CP-CML) (A, $n = 5$) or blast phase CML (BP-CML)/tyrosine kinase inhibitor (TKI)-resistant (B, $n = 3$) patients were lentivirally transduced for ectopic G0S2 expression followed by colony formation (left) and apoptosis (right) assays. (C and D) Primary CD34⁺ cells isolated from normal cord blood (CB) ($n = 3$) were lentivirally transduced for G0S2 ectopic expression (C) or knockdown (D) followed by colony formation (left) and apoptosis (right) assays. Error bars represent standard error of the mean (SEM). EV, empty vector; IM, imatinib

apoptosis in newly diagnosed CP-CML CD34⁺ cells (Figure 3A, right). However, ectopic G0S2 restored imatinib sensitivity in cells from myeloid BP-CML patients (Figure 3B, right). In normal CB CD34⁺ cells, neither G0S2 ectopic expression nor knockdown had any effect on colony formation or apoptosis (Figure 3C,D). Altogether, these data implicate a tumour suppressor role for G0S2 in CML disease progression and TKI resistance.

3.4 | Altered G0S2 expression impairs growth of CML cells in vivo

In a previous report, ectopic G0S2 expression reduced subcutaneous tumour formation by K562 cells in vivo, and we confirmed these findings (Figure 4A).⁴³ To assess the role of murine G0s2 in mouse models, we ectopically expressed p210^{BCR::ABL1} in murine 32Dcl3 myeloid progenitors or lineage-negative mouse BM. In contrast with our data in human CB CD34⁺ cells (Figure 1F), enforced BCR::ABL1 expression in murine cells increased *G0s2* mRNA but not

protein expression (Figure 4B,C). This is not surprising, as introduction of BCR::ABL1 into murine myeloid progenitors is known to induce cell cycle progression,^{50,51} and *G0s2* was first identified as a gene that is upregulated during G0-to-G1 cell cycle transition in murine MNCs, hence its name.^{52,53} Consistent results were observed in lineage-negative mouse BM cells transduced with p210^{BCR::ABL1} (Figure 4D). To assess the in vivo effects of G0s2 loss in CML, we utilised lineage-negative BM from wild-type versus *G0s2*^{-/-} mice, and performed a retroviral transduction/transplantation assay that mimics BP-CML. Ablation of G0s2 protein in the lineage-negative BM fraction of *G0s2*^{-/-} mice was confirmed by immunoblot (Figure 4E). In untransformed cells, we observed a 35% reduction of colony formation in lineage-negative *G0s2*^{-/-} BM cells compared with wild-type controls (Figure 4F). Similar effects were observed in 32Dcl3 cells expressing shRNA targeting G0s2 (shG0s2) cultured in murine IL-3, with a greater reduction of colony formation in cells cultured with mG-CSF (Figure S4A). When we transduced lineage-negative BM cells with p210^{BCR::ABL1}, loss of G0s2 resulted

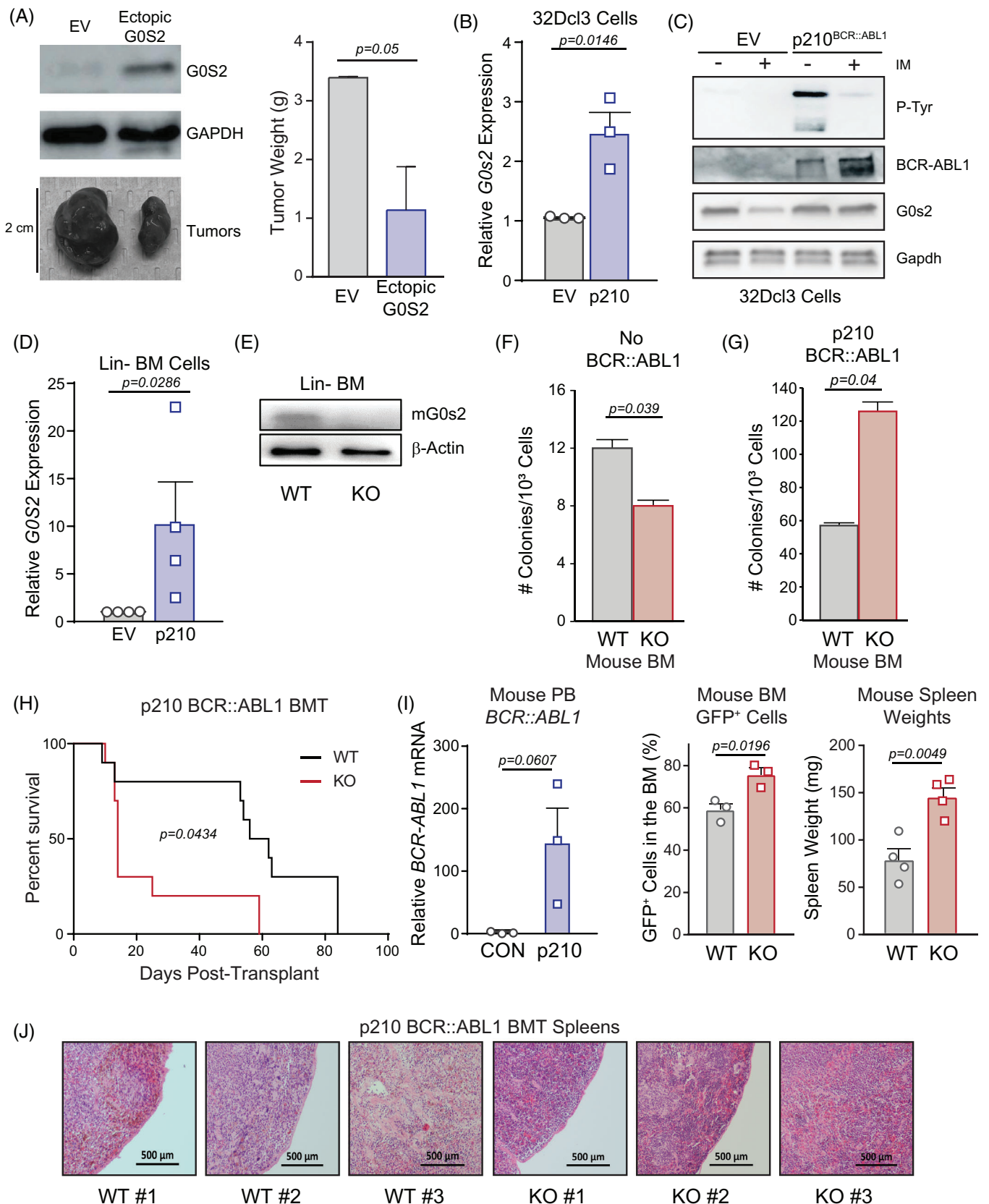


FIGURE 4 Altered G0/G1 switch gene 2 (G0S2) expression impairs growth of chronic myeloid leukaemia (CML) cells in vivo. (A) K562 cells were lentivirally transduced for ectopic G0S2 expression versus the empty vector (EV) control, and 3×10^6 resulting cells were injected subcutaneously into the rear flanks of 6–8-week-old nude mice ($n = 3$ per group). Image shows relative size of subcutaneous tumours excised from recipient mice, and immunoblot analyses confirmed ectopic G0S2 expression at the protein level in vivo. Bar graph shows the tumour

in a significant increase in colony formation compared with controls (Figure 4G). Consistently, we observed a significant reduction in overall survival comparing recipients of $G0s2^{-/-}$ versus wild-type BM expressing the p210^{BCR::ABL1} oncoprotein (Figure 4H). Confirming that our recipient mice indeed died of leukaemia, *BCR::ABL1* transcripts were detectable in the peripheral blood of recipient mice but not controls (Figure 4I, left). Additionally, the percentage of GFP⁺ cells in the BM of moribund mice was higher in $G0s2^{-/-}$ compared with wild-type recipients (Figure 4I, middle), which correlated with increased splenomegaly (Figure 4I, right) and splenic cellularity (Figure 4J). Altogether, loss of *G0S2* expression reduced overall survival in both CP-CML patients (Figure 1F) and murine models of CML (Figure 4H–J).

3.5 | *G0S2* expression correlates with myeloid development and is downregulated in the CML GMP population

The reduction of colonies in 32Dcl3-sh*G0s2* cells cultured in mG-CSF (Figure S4A, right) suggested a role for *G0s2* in myeloid differentiation. Consistently, differentiation of 32Dcl3 cells in the presence of mG-CSF markedly upregulated *G0S2* expression, but not in cells expressing p210^{BCR::ABL1} (Figure S4B). 32Dcl3-sh*G0s2* cells cultured in mG-CSF and doxycycline demonstrated a block of differentiation upon morphologic examination (Figure S4C). Similar results were observed in lineage-negative BM from $G0s2^{-/-}$ compared with wild-type mice cultured in mG-CSF (Figure 5A,B). These data suggest that *G0S2* expression is associated with myeloid development. Consistently, pathway enrichment analysis of the genes co-expressed with *G0S2* in CML¹² revealed neutrophil degranulation as the top dysregulated pathway (>12 FC, Figure S5A,B). We performed complete blood counts (CBCs) on peripheral blood of wild-type versus $G0s2^{-/-}$ mice, and observed

a significant reduction in only the percentage of neutrophils, with a concomitant increase in lymphocytes (Figure S6A,B). Reduced peripheral blood neutrophils in $G0s2^{-/-}$ mice were confirmed upon visual inspection of blood smears stained with Wright–Giemsa for morphology (Figure S6C). Yamada et al. reported that *G0s2* expression in mice was highest in the most primitive HSC population, and lowest in terminally differentiated cells.¹⁴ However, using Gene Expression Commons, a compilation of thousands of microarray datasets, murine *G0s2* mRNA expression was lowest in primitive populations, and highest in mature granulocytes, lymphocytes and natural killer cells (Figure S6D). Data from BloodSpot confirmed these results in murine haematopoietic cells (Figure S6E).^{54–56} Consistently, RT-qPCR experiments revealed that *G0s2* mRNA expression was undetectable in purified murine long-term HSCs (LT-HSCs) and short-term HSCs (ST-HSCs) compared with the bulk lineage-negative fraction (Figure 5C). While *G0S2* is an ATRA target gene in APL,²³ little is known about *G0S2* expression in human stem/progenitor cells.

Consistent with the murine data, analysis of several human datasets demonstrated low *G0S2* expression in primitive HSCs, and high *G0S2* in mature granulocytes, monocytes and CD4⁺ T cells (Figure S6F).^{57–61} Accordingly, *G0S2* mRNA expression was upregulated in peripheral blood CD14⁺ monocytes from human G-CSF-mobilised versus untreated individuals (GSE1746, Figure 5D). Differentiation of CB CD34⁺ cells with hG-CSF, or THP-1 cells with phorbol 12-myristate 13-acetate, increased *G0S2* expression (Figure 5E,F). To characterise *G0S2* expression in human haematopoietic stem/progenitor cells, we sorted CD34⁺ cells by FACS for GMPs, CMPs, MEPs, MPPs, or HSCs, and measured *G0S2* expression by RT-qPCR. In CML versus normal CD34⁺ cells, *G0S2* mRNA expression was universally low in HSCs from normal individuals and in LSCs from CP-CML patients. Our data revealed a loss of *G0S2* expression exclusively within the GMP population (Figure 5G). Thus,

weight (g) for $n = 3$ replicates of the experiment. (B and C) Reverse transcription-quantitative polymerase chain reaction (RT-qPCR) (B) and immunoblot (C) analyses demonstrate murine *G0s2* mRNA and protein levels, respectively, in 32Dcl3 myeloid precursors upon ectopic expression of p210^{BCR::ABL1}. (D) Similarly, RT-qPCR shows *G0s2* mRNA in lineage-negative mouse bone marrow (BM) upon ectopic expression of p210^{BCR::ABL1}. (E) Immunoblot shows murine *G0s2* protein levels in lineage-negative mouse BM from wild-type (WT) versus $G0s2^{-/-}$ [knockout (KO)] mice. β -Actin was assessed as a loading control. (F and G) Lineage-negative mouse BM from WT or $G0s2^{-/-}$ mice were either plated directly in colony formation assays (F) or were retrovirally transduced with p210^{BCR::ABL1} followed by plating in colony formation assays (G). Bar graphs represent the number of colonies per 1000 cells. (H) Lineage-negative mouse BM from WT or $G0s2^{-/-}$ mice were retrovirally transduced with p210^{BCR::ABL1} followed by intravenous injection into lethally irradiated recipients ($n = 10$ per group). Survival over time is shown in the Kaplan–Meier curve. (I) RT-qPCR confirmed *BCR::ABL1* mRNA expression in the peripheral blood of recipient mice (left). Bar graphs show GFP⁺BCR::ABL1⁺ cells comparing recipients of WT versus $G0S2^{-/-}$ BM cells (middle), as well as spleen weights of moribund mice after euthanasia (right). (J) Images show spleen morphology as assessed by haematoxylin and eosin staining at 4 weeks post-transplant ($n = 3$ per group). Error bars represent standard error of the mean (SEM). BMT, bone marrow transplantation; EV, empty vector; PB, peripheral blood

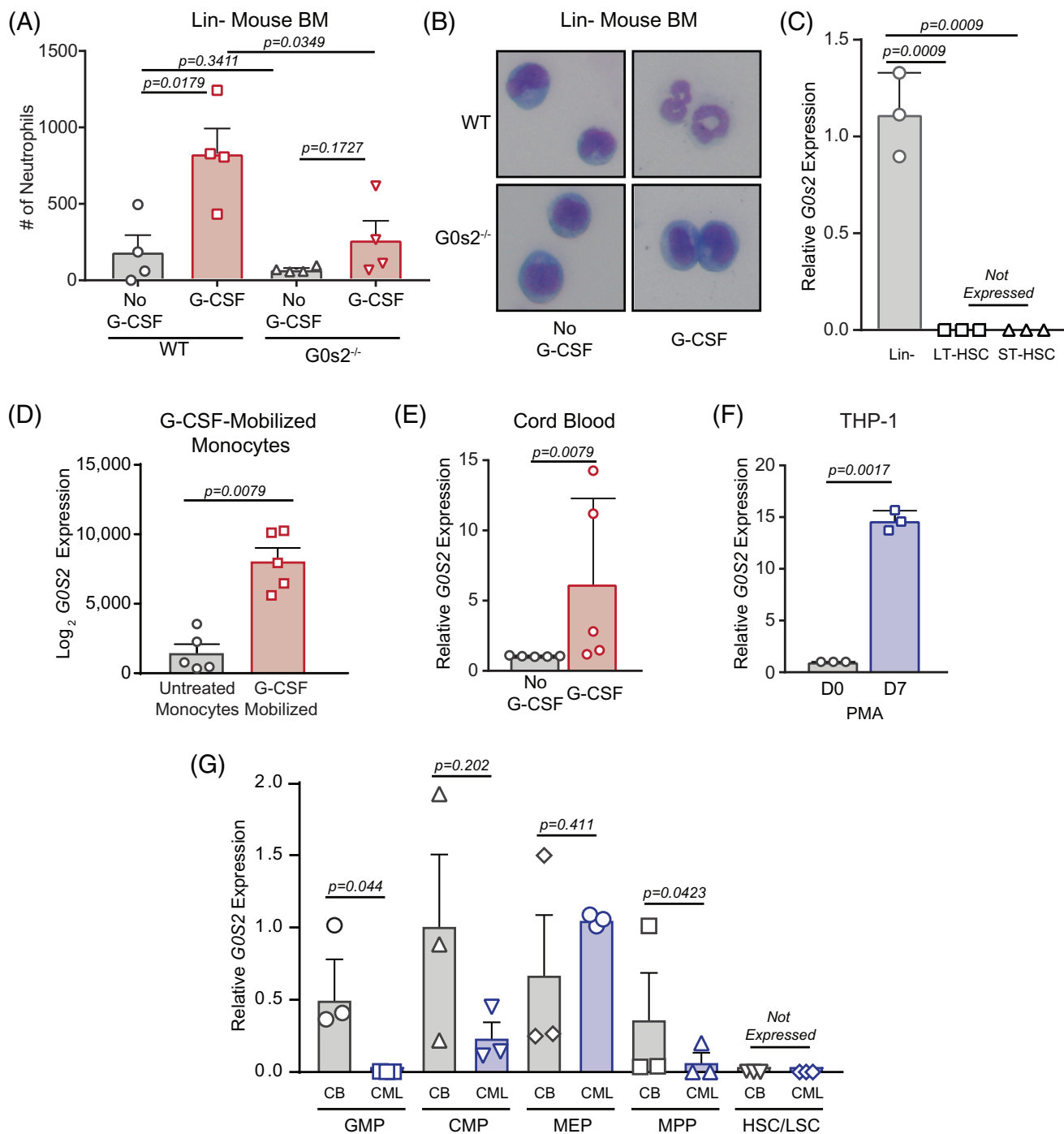


FIGURE 5 G0/G1 switch gene 2 ($G0S2$) expression correlates with myeloid development, and reduced expression in chronic myeloid leukaemia (CML) occurs within the granulocyte–macrophage progenitor (GMP) population. (A and B) Bar graph shows the number (#) of neutrophils counted in Wright–Geimsa stains of lineage-negative (Lin^{-}) mouse bone marrow (BM) from wild-type or $G0s2^{-/-}$ mice induced towards neutrophil differentiation with murine granulocyte-colony stimulating factor (mG-CSF) (A). The image shows representative morphology for the indicated treatment conditions (B). (C) Bar graph represents relative $G0s2$ mRNA expression in the bulk Lin^{-} BM fraction compared with sorted long-term (LT) and short-term (ST) haematopoietic stem cells (HSCs) ($n = 3$). (D) Bar graph shows $G0S2$ mRNA expression in haematopoietic cells after in vivo mobilisation with G-CSF for 7 days (GSE1746, $n = 5$). (E and F) Bar graphs show $G0S2$ mRNA expression in cord blood (CB) $CD34^{+}$ cells induced to differentiate with human G-CSF (hG-CSF) (E, $n = 5$), or THP-1 cells induced to differentiate with phorbol 12-myristate 13-acetate (PMA) for 7 days (F, $n = 3$). (G) Bar graph shows relative $G0S2$ mRNA expression in $CD34^{+}$ cells from normal CB ($n = 3$, left) or chronic phase CML (CP-CML) patients ($n = 3$, right) that were sorted for GMPs, common myeloid progenitors (CMPs), megakaryocyte–erythrocyte progenitors (MEPs), multipotent progenitors (MPPs) or HSCs based on cell surface molecule expression. $G0S2$ mRNA expression was universally low in normal HSCs and CP-CML leukaemic stem cells (LSCs), and significantly reduced in CP-CML versus CB GMPs. Error bars represent standard error of the mean (SEM).

the reduction of *G0S2* expression observed in CML CD34⁺ cells (Figure 1A) is due to GMPs, the disease-causing population in BP-CML.⁶² Altogether, these data suggest that loss of *G0S2* expression (Figure 1A) promotes the blockade of differentiation observed in BP-CML patients.^{63,64}

3.6 | The *G0S2* inhibitory effect on cell survival is independent of adipose triglyceride lipase

Loss of *G0S2* expression in CML GMPs could mark a block of differentiation that promotes TKI resistance, similar to previous reports.^{4,65} Gianni et al.⁶⁶ recently published a role for lipid metabolism during ATRA-induced differentiation of the NB4 APL cell line. It is well known that *G0S2* binds to and inhibits adipose triglyceride lipase (ATGL), the rate-limiting enzyme for intracellular lipolysis,^{17,20} and *G0S2*-mediated ATGL inhibition was reported to attenuate the growth of cancer cells.⁶⁷ Lipolysis refers to the hydrolysis of triacylglycerols (TAGs) into their constituent components, including glycerol and free fatty acids (Figure S7A).^{17,18} TAG fat depots are used for a number of purposes, including thermogenesis (heat), energy (fatty acid beta-oxidation) and insulation.⁶⁸ However, to date, the role of ATGL in CML has not been explored. Since *G0S2* is an ATGL inhibitor, we hypothesised that ATGL knockdown (shATGL) would mimic ectopic *G0S2* expression (Figure 3), but this was not the case. RNAseq on K562^S cells expressing ectopic *G0S2* versus shATGL showed a clear separation between groups, but shATGL-expressing cells did not cluster with ectopic *G0S2* (Figure S8). Gene Ontology (GO) analysis of the genes dysregulated by ectopic *G0S2* expression versus ATGL knockdown did not reveal concordant pathways (Figure 6A). ATGL protein is readily expressed in K562 cells, and its expression is independent of BCR::ABL1 kinase activity (Figure S7B). *G0S2* ectopic expression or knockdown had no effect on ATGL protein levels in K562 cells (Figure 6B). Surprisingly, shATGL (Figure S7C) increased survival with no effect on apoptosis in K562^S cells and another CML cell line, KU812 (Figures 6C and S7D,E). When we ectopically expressed *G0S2* upon simultaneous ATGL knockdown (Figure 6D), the phenotype in colony formation assays mimicked ectopic *G0S2* alone, reducing colony formation by ~50% (Figure 6E, left). However, ATGL knockdown combined with ectopic *G0S2* expression increased imatinib-mediated apoptosis (Figure 6E, right), similar to our observations in BP-CML CD34⁺ cells upon ectopic *G0S2* expression (Figure 3B right). Accordingly, *ATGL* mRNA was downregulated in BP-CML versus CP-CML or AP-CML (Figure 6F) by RNAseq. mRNA encoding two other enzymes in the lipolytic pathway, hormone-sensitive

lipase and monoacylglycerol lipase, showed a similar trend (Figure 6G,H). These data suggest downregulation of lipolytic genes during CML disease progression, and that ATGL activity suppresses *G0S2*-mediated apoptosis in the presence of imatinib.

3.7 | Loss of *G0S2* expression in CML disrupts glycerophospholipid metabolism

Thus far, our data implicate ATGL-dependent functions for *G0S2* in apoptosis of CML, and ATGL-independent functions for *G0S2* in survival of CML. The top GO pathways regulated by ectopic *G0S2* expression in K562 cells included receptor complex, side of membrane and regulation of lipid localisation, among others (Figure 6A, right). Pathway enrichment analysis of differentially expressed genes comparing *G0S2* ectopic expression versus knockdown in K562 cells revealed various pathways of interest. Notably, long-chain fatty acid metabolism and other lipid pathways were upregulated in cells expressing ectopic *G0S2* and downregulated in sh*G0S2*-expressing cells (Figure 7A). Therefore, we assessed those cells for changes in lipid species by untargeted LC/MS-based lipidomics. Analysis of lipids altered by *G0S2* revealed mono-, di- and triglycerides, as expected,^{17,19,20} which were reduced by sh*G0S2* and increased by ectopic *G0S2* (Figure 7B,C). We also observed increased levels of long-chain but not short-chain phosphatidylcholines and phosphatidylethanolamines upon ectopic *G0S2* expression (Figure 7C). In fact, the most significantly different lipid categories between groups primarily included members of the glycerophospholipid family (Figures 7D and S9A,B). Glycerophospholipids consist of a polar head group attached to a glycerol backbone that includes up to two fatty acyl chains. Glycerophospholipids are characterised based on the composition of their polar head groups, including phosphatidylcholine, phosphatidylethanolamine, phosphatidylinositol, phosphatidylserine, phosphatidylglycerol and cardiolipin, and they are found mostly in membranes where they control fluidity, stability and permeability.⁶⁹ Additional pathways regulated by *G0S2* in K562 cells included autophagy, glycosylphosphatidylinositol (GPI)-anchor biosynthesis, ferroptosis and choline metabolism in cancer (Figure S9A,B). Consistent with the reported enzymatic activity of *G0S2*,¹⁹ the phosphatidic acid PA(22:6_22:1)-H was the top most differentially expressed lipid comparing *G0S2* ectopic expression versus knockdown, with a 3.2-fold increase in cells expressing ectopic *G0S2*. Thus, we focused our attention on the genes involved with these pathways in our RNAseq data. As shown in Figure S9C–H, the genes encoding acyl-Co-A synthetase long-chain family

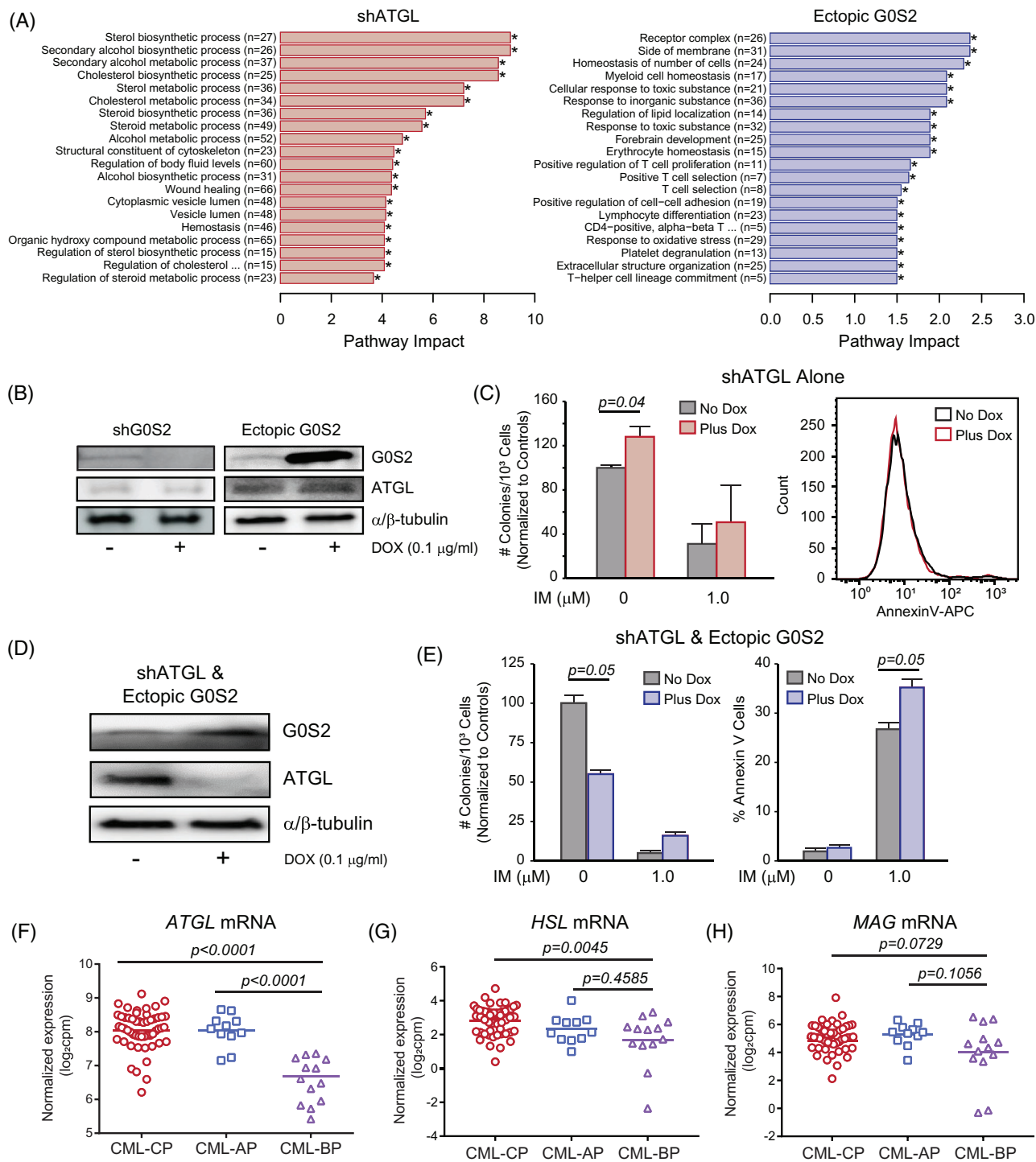


FIGURE 6 The effect of G0/G1 switch gene 2 (G0S2) on survival is independent of its known function as an inhibitor of adipose triglyceride lipase (ATGL). (A) Bar graphs show Gene Ontology (GO) analysis for the pathways dysregulated in K562^S cells upon ATGL knockdown (left) or ectopic G0S2 expression (right) compared with controls by RNA sequencing ($n = 2$). * $p < .05$. (B) Immunoblots show G0S2 and ATGL protein levels in K562^S cells upon ectopic G0S2 expression or knockdown \pm doxycycline (DOX) (0.1 $\mu\text{g}/\text{ml}$, 72 h). α/β -Tubulin was assessed as a loading control. (C) Bar graph represents colony forming ability of K562-shATGL cells \pm DOX and \pm imatinib (IM) (1 μM , left). The representative histogram shows the effect of shATGL on apoptosis of K562 cells in vitro (right). (D and E) K562^S cells were engineered for simultaneous DOX-inducible ATGL knockdown and ectopic G0S2 expression. Protein levels were confirmed by immunoblot analysis (D) and subject to colony formation (E, left) and apoptosis assays (E, right). (F and H) Dot plots from RNA sequencing data demonstrated reduced ATGL (F), hormone-sensitive lipase (HSL) (G) and monoacylglycerol lipase (MAG) (H) mRNA levels in mononuclear cells from blast phase chronic myeloid leukaemia (BP-CML) ($n = 14$) compared with chronic phase CML (CP-CML) ($n = 53$) and/or accelerated phase CML (AP-CML) ($n = 11$) patients. Error bars represent standard error of the mean (SEM).

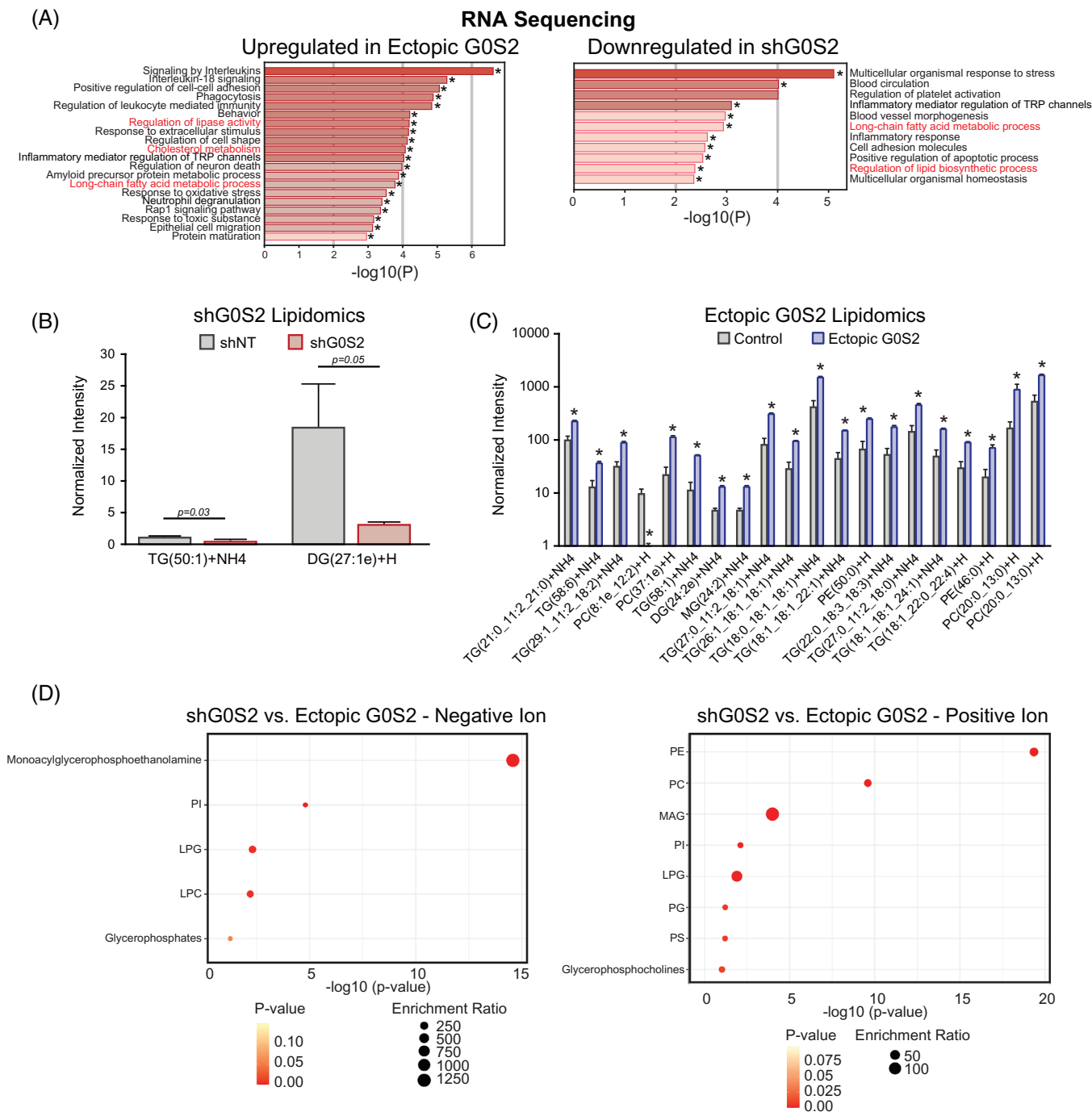


FIGURE 7 Loss of G0/G1 switch gene 2 (G0S2) expression in chronic myeloid leukaemia (CML) promotes the accumulation of very long-chain unsaturated fatty acids and altered glycerophospholipid metabolism. (A) Bar graphs show Gene Ontology (GO) analysis for the pathways that are upregulated upon G0S2 ectopic expression (left) or downregulated upon G0S2 knockdown (right) in K562^S cells by RNA sequencing. * $p < .05$. Consistent pathways are indicated in red. (B and C) K562 cells expressing either the non-targeting control vector (shNT), shRNA targeting G0S2 (shG0S2), or ectopic G0S2 were analysed by untargeted liquid chromatography (LC)/mass spectrometry (MS)-based lipidomics. shG0S2 resulted in a reduction of very long-chain di- and triglycerides (B). Ectopic G0S2 promoted the accumulation of triglycerides as well as several cell membrane components, including phosphatidylcholine (PC) and phosphatidylethanolamine (PE) species (C). (D) Lipid pathway enrichment was performed based on KEGG databases comparing K562^S cells with G0S2 ectopic expression or knockdown. DAG, diacylglycerol; LPC, lysophosphatidylcholine; LPG, lysophosphatidylglycerol; MAG, monoacylglycerol; PG, phosphatidylglycerol; PI, phosphatidylinositol; PS, phosphatidylserine; TAG, triacylglycerol

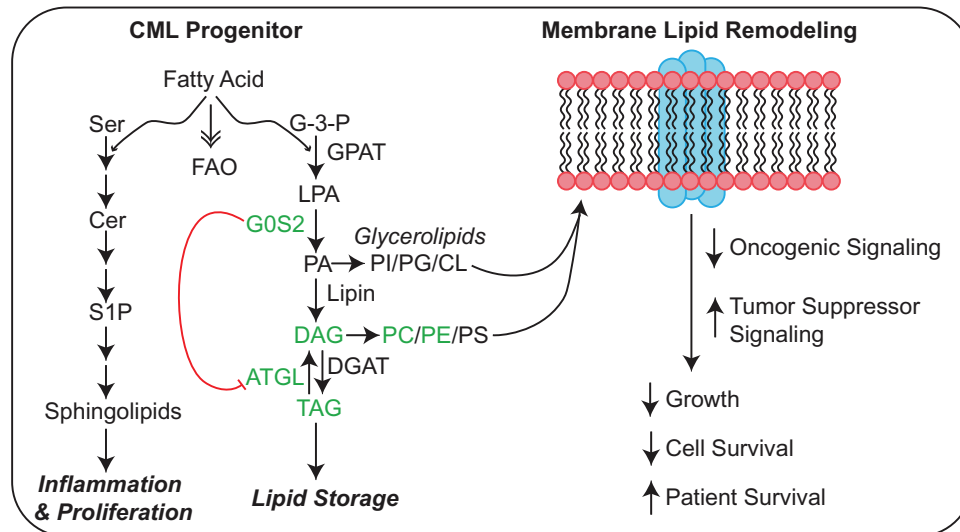


FIGURE 8 Proposed model for G0/G1 switch gene 2 (*G0S2*) tumour suppressor activity in chronic myeloid leukaemia (CML). The schematic shows the effect of *G0S2* on triacylglyceride (TAG) accumulation both indirectly through adipose triglyceride lipase (ATGL) inhibition, and directly through lysophosphatidic acid acyltransferase (LPAAT) activity. As ectopic *G0S2* resulted in the accumulation of diacylglycerides (DAGs), TAGs, and species of phosphatidylcholine (PC) and phosphatidylethanolamine (PE) (Figure 7), our data suggest that *G0S2* contributes to lipid homeostasis either by increasing TAG stores or by inducing membrane lipid remodelling. Pathway enrichment analysis of our K562 lipidomics data demonstrated that the lipid pathways affected most by differential *G0S2* expression included glycerophospholipid metabolism, autophagy, glycosylphosphatidylinositol (GPI)-anchor biosynthesis, ferroptosis and choline metabolism in cancer (Figure S9A,B). However, more work needs to be done to determine where these lipid species are being incorporated.

member 1 (ACSL1), butyrylcholinesterase (BCHE), lysophosphatidylcholine acyltransferase 1 (LPCAT1), lysophosphatidylcholine acyltransferase 2 (LPCAT2) and phosphatidylcholine transfer protein (PCTP) were upregulated by ectopic *G0S2* expression (Figure S9C–G). Conversely, the gene encoding the CD36 fatty acid transporter was downregulated by ectopic *G0S2* expression (Figure S9H). Altogether, our data imply that loss of *G0S2* expression in CML disrupts lipid homeostasis, particularly glycerophospholipid metabolism, resulting in a block of differentiation that renders cells resistant to TKI therapy (Figure 8).

4 | DISCUSSION

BCR::ABL1-positive CML is a clonal haematologic malignancy that is functionally curable through treatment with TKIs targeting BCR::ABL1.⁷⁰ While TKI-mediated BCR::ABL1 inhibition has revolutionised CML therapy, resistance remains a problem, and TKIs do not target the CML LSC population, requiring lifelong TKI therapy for the majority of patients.⁴ While second- and third-generation TKIs were developed to combat TKI resistance, treatment-free remission is still unattainable for many CML patients.^{9,70} In the present study, we elucidated a role for *G0S2* as a tumour suppressor in CML that is downregu-

lated in multiple scenarios of TKI resistance, including TKI non-responders versus responders (Figure 1A,D), BP-CML versus CP-CML (Figure 1A,C), and CP-CML versus normal myeloid progenitors (Figure 5G). Therefore, primary TKI resistance and blastic transformation of CML may involve biologically similar pathways, as recently reported by Zhao et al.³⁵ Low levels of *G0S2* mRNA correlated with worse overall survival for both CML patients (Figure 1E) and in mouse models of the disease (Figure 4H–J). *G0S2* downregulation in CML was not a result of promoter hypermethylation or BCR::ABL1 kinase activity, but was rather due to transcriptional repression by MYC (Figure 2). However, we cannot rule out the possibility that loss of transcription factor expression, such as CCAAT enhancer binding protein beta (*C/EBPβ*)^{71,72} or peroxisome proliferator-activated receptor gamma (*PPARγ*),^{73,74} may also play a role in reduced *G0S2* expression during CML disease progression and TKI resistance. Both *CEBPβ* and *PPARγ* are known to regulate *G0S2* expression in murine BM adipocytes.^{16,75–77} Ultimately, our data identified a tumour suppressor role for *G0S2* in CML survival and TKI resistance that was independent from its canonical function as an inhibitor of ATGL.

G0s2^{-/-} mice are born at a normal Mendelian ratio³²; however, offspring of *G0s2*^{-/-} mothers do not survive 48 h due to lactation defects.³² Consistent with the role of *G0S2* in lipolysis,^{17,18} mice lacking *G0s2* have defects

in lactation, energy balance and thermogenesis.³² G0S2 function traditionally relies on protein–protein interactions, such as BCL-2,¹³ ATGL^{17,67} or nucleolin,^{14,43} and G0S2-mediated ATGL inhibition was shown to attenuate the growth of cancer cells.⁶⁷ Although G0S2 expression alone in this study had no effect on apoptosis of CML cells, G0S2 increased imatinib-mediated apoptosis when ATGL expression was low (BP-CML, Figure 3B; shATGL, Figure 6E), implying that ATGL abrogates the effects of G0S2 on apoptosis. ATGL-mediated lipolysis was shown to activate the NAD⁺-dependent deacetylase, sirtuin 1 (SIRT1),⁷⁸ which regulates metabolism and leukemogenic potential in CML LSCs.^{79–82} Thus, it is possible that ATGL-mediated SIRT1 activation could be responsible for abolishing G0S2-mediated apoptosis in scenarios when it is highly expressed (e.g., CP-CML). Importantly, a recent report identified an enzymatic function for G0S2 in liver hepatocytes that is independent of protein–protein interactions. These data demonstrated for the first time that G0S2 has the ability to mediate phosphatidic acid (PA) synthesis from lysophosphatidic acid and acyl-coenzyme A, known as lysophosphatidic acid acyltransferase (LPAAT) activity.¹⁹ In fact, our lipidomics data on K562 cells demonstrated that PA(22:6_22:1)-H was the top most differentially expressed lipid comparing G0S2 ectopic expression versus knockdown. Pathway enrichment analysis of our K562 lipidomics data demonstrated that the lipid pathways affected most by differential G0S2 expression included glycerophospholipid metabolism, autophagy, GPI-anchor biosynthesis, ferroptosis and choline metabolism in cancer (Figure S9A,B). Importantly, ectopic G0S2 expression resulted in the accumulation of long- and very long-chain unsaturated fatty acids in CML (Figure 7C). A recent study by Liu et al. reported that long-chain acyl-CoA synthetase 1 (ACSL1) overexpression enhanced the proliferation-inhibiting effects of imatinib in CML cells.⁸³ Consistently, our data suggest that *ACSL1* gene expression is upregulated by G0S2 ectopic expression in CML (Figure S8A), and therefore may play a role in its tumour suppressor activity during CML disease progression and TKI response. Future studies will explore the role of G0S2 LPAAT activity in normal and leukaemic haematopoiesis to better understand the function of G0S2 and lipid metabolism in the haematopoietic system.

G0S2 was reported to maintain quiescence of murine HSCs by sequestering nucleolin in the cytosol, thereby preventing its pro-proliferation functions in the nucleus.^{14,15} However, our data and publicly available data show that G0S2 expression is lowest in primitive HSCs, and highest in cells committed towards the myeloid lineage (Figures 5 and S4–S6). While ectopic G0S2 binding to nucleolin could explain the reduced survival we observed in CML cells in vitro, it cannot play a role in human HSCs because

G0S2 is not expressed. Rather, loss of G0S2 expression in the GMP population predicts a block of differentiation that renders CML cells resistant to therapy. Thus, our data indicate that differentiation blockade is a unifying feature of BCR::ABL1-independent TKI resistance, and suggest that promoting differentiation can enhance TKI responsiveness.

A major strength of our study is the use of primary CML specimens and animal models to establish G0S2 expression levels and phenotypes during CML disease progression and TKI resistance. Limitations to our study include the heavy reliance on CML cell lines for the functional and metabolic analyses. Future studies will assess the functional role of altered lipid metabolism in primary CML patient specimens and mouse models. Altogether, our data implicate G0S2 as a regulator of both myeloid differentiation and lipid metabolism pathways (Figures 5, 7 and S4–S6). RNAseq data in the current study revealed that G0S2 regulates pathways involved in fatty acid metabolism in CML, which was confirmed by LC/MS-based lipidomics analyses (Figure 7). Thus, the role of G0S2 as a tumour suppressor in CML and in normal myeloid differentiation could depend on its LPAAT enzymatic activity and the ability to synthesise PA (Figure 8), which will be the topic of future investigation. Our data also imply that loss of G0S2 expression in CML is in part due to the MYC oncoprotein. MYC is a well-known regulator of metabolic reprogramming in cancer,⁴⁵ including lipid metabolism.⁴⁴ Interestingly, lipid metabolism was recently reported to regulate ATRA-induced differentiation of APL cells.⁶⁶ In this study, Gianni et al. revealed that exposure of APL cells to ATRA caused an early reduction of cardiolipins, a lipid component found primarily in mitochondrial membranes.⁶⁶ This decrease in cardiolipins was associated with inhibition of mitochondrial activity during ATRA-induced myeloid differentiation, which they observed in ATRA-sensitive but not ATRA-resistant APL cells.⁶⁶ Furthermore, lysophospholipid metabolism was recently reported to be essential for CML LSC survival.^{84,85} Naka et al. demonstrated that the *Gdpd3* gene, which encodes the lysophospholipase D enzyme, is more highly expressed in murine CML stem cells compared with wild-type HSCs, and that *Gdpd3*-deficient CML stem cells have impaired self-renewal capabilities.^{84,85} In our study, altered G0S2 expression in CML changed the expression of di- and tri-glycerides, but also several glycerophospholipids, including phosphatidylcholine and phosphatidylethanolamine (Figure 7). These changes correlated with alterations in the expression of several enzymes involved in choline metabolism, including *ACSL1*, *BCHE*, *LPCAT1/2* and *PCTP* (Figure S9). However, more work needs to be done to determine where these lipid species are being incorporated. Are they going to the cell membrane, lysosomal membranes

(e.g., autophagy), endoplasmic reticulum membranes or mitochondrial membranes? Could they be contributing to enhanced mitochondrial fatty acid beta-oxidation? These are all topics of current and future investigation in our laboratory, in order to better understand the role of lipid metabolism in CML stem cell survival and TKI response. As lipid-modifying drugs were recently shown to enhance molecular response in CML patients on TKI therapy,⁸⁶ our data suggest that restoring G0S2 expression and/or lipid-modifying drugs could have clinical utility by improving lipid homeostasis, promoting myeloid differentiation and reestablishing TKI sensitivity.


ACKNOWLEDGEMENTS

The authors would like to thank Ethan Dmitrovsky, MD, for providing the G0s2^{-/-} mice that were used in this study. We also thank Michael Deininger, MD, PhD, from the University of Utah Huntsman Cancer Institute, for providing the cell lines and patient samples used in this study. Research reported in this publication was supported by the National Cancer Institute of the National Institutes of Health under award numbers K22CA216008 (A. M. E.) and R01CA065823 (B. J. D.). The content is solely the responsibility of the authors and does not necessarily represent the official views of the National Institutes of Health. Research was also funded in part through the Seed Grant Funding to Catalyse UTEP-TTUHSC El Paso Joint Research Funding Projects program.

CONFLICTS OF INTEREST

B.J.D. serves on scientific advisory boards for Aileron Therapeutics, Therapy Architects (ALLCRON), Cepheid, Vivid Biosciences, Celgene, RUNX1 Research Program, Novartis, Gilead Sciences (inactive), Monojul (inactive); serves on Scientific Advisory Boards and receives stock from Aptose Biosciences, Blueprint Medicines, EnLiven Therapeutics, Iterion Therapeutics, Third Coast Therapeutics, GRAIL (inactive on scientific advisory board); is scientific founder of MolecularMD (inactive, acquired by ICON); serves on the board of directors and receives stock from Amgen, Vincer Pharma; serves on the board of directors for Burroughs Wellcome Fund, CureOne; serves on the joint steering committee for Beat AML LLS; is founder of VB Therapeutics; has a sponsored research agreement with EnLiven Therapeutics; receives clinical trial funding from Novartis, Bristol-Myers Squibb, Pfizer. The remaining authors have no competing financial interests.


ORCID

Mayra A. Gonzalez  <https://orcid.org/0000-0002-7980-6685>

Idaly M. Olivas  <https://orcid.org/0000-0001-9039-5322>

Alfonso E. Bencomo-Alvarez  <https://orcid.org/0000-0002-1771-8532>

Christian Barreto-Vargas  <https://orcid.org/0000-0002-5229-611X>

Katherine E. Varley  <https://orcid.org/0000-0003-1622-5290>

Brian J. Druker  <https://orcid.org/0000-0001-8331-8206>

Md Nurunnabi  <https://orcid.org/0000-0003-4457-3401>

Sudip Bajpeyi  <https://orcid.org/0000-0002-5336-8330>

Anna M. Eiring  <https://orcid.org/0000-0001-6533-9150>

REFERENCES

1. Nowell PC, Hungerford D. A minute chromosome in human chronic granulocytic leukemia. *Science*. 1960;132:1497.
2. Druker BJ, Guilhot F, O'Brien SG, et al. Five-year follow-up of patients receiving imatinib for chronic myeloid leukemia. *N Engl J Med*. 2006;355(23):2408-2417.
3. Calabretta B, Perrotti D. The biology of CML blast crisis. *Blood*. 2004;103(11):4010-4022.
4. O'Hare T, Zabriskie MS, Eiring AM, Deininger MW. Pushing the limits of targeted therapy in chronic myeloid leukaemia. *Nat Rev Cancer*. 2012;12(8):513-526.
5. Graham SM, Jorgensen HG, Allan E, et al. Primitive, quiescent, Philadelphia-positive stem cells from patients with chronic myeloid leukemia are insensitive to STI571 in vitro. *Blood*. 2002;99(1):319-325.
6. Corbin AS, Agarwal A, Loriaux M, Cortes J, Deininger MW, Druker BJ. Human chronic myeloid leukemia stem cells are insensitive to imatinib despite inhibition of BCR-ABL activity. *J Clin Invest*. 2011;121(1):396-409.
7. Mahon FX, Rea D, Guilhot J, et al. Discontinuation of imatinib in patients with chronic myeloid leukaemia who have maintained complete molecular remission for at least 2 years: the prospective, multicentre Stop Imatinib (STIM) trial. *Lancet Oncol*. 2010;11(11):1029-1035.
8. Mahon FX. Discontinuation of TKI therapy and 'functional' cure for CML. *Best Pract Res Clin Haematol*. 2016;29(3):308-313.
9. Mahon FX. Treatment-free remission in CML: who, how, and why? *Hematology Am Soc Hematol Educ Program*. 2017;2017(1):102-109.
10. Cortes JE, Kim DW, Pinilla-Ibarz J, et al. A phase 2 trial of ponatinib in Philadelphia chromosome-positive leukemias. *N Engl J Med*. 2013;369(19):1783-1796.
11. Holyoake TL, Vetrie D. The chronic myeloid leukemia stem cell: stemming the tide of persistence. *Blood*. 2017;129(12):1595-1606.
12. McWeeney SK, Pemberton LC, Loriaux MM, et al. A gene expression signature of CD34+ cells to predict major cytogenetic response in chronic-phase chronic myeloid leukemia patients treated with imatinib. *Blood*. 2010;115(2):315-325.
13. Welch C, Santra MK, El-Assaad W, et al. Identification of a protein, G0S2, that lacks Bcl-2 homology domains and interacts with and antagonizes Bcl-2. *Cancer Res*. 2009;69(17):6782-6789.
14. Yamada T, Park CS, Burns A, Nakada D, Lacorazza HD. The cytosolic protein G0S2 maintains quiescence in hematopoietic stem cells. *PLoS One*. 2012;7(5):e38280.

15. Yu Z, Yang W, He X, et al. Endothelial cell-derived angiopoietin-like protein 2 supports hematopoietic stem cell activities in bone marrow niches. *Blood*. 2022;139(10):1529-1540.
16. Choi H, Lee H, Kim TH, et al. G0/G1 switch gene 2 has a critical role in adipocyte differentiation. *Cell Death Differ*. 2014;21(7):1071-1080.
17. Yang X, Lu X, Lombes M, et al. The G(0)/G(1) switch gene 2 regulates adipose lipolysis through association with adipose triglyceride lipase. *Cell Metabol*. 2010;11(3):194-205.
18. Zhang X, Heckmann BL, Campbell LE, Liu J. G0S2: a small giant controller of lipolysis and adipose-liver fatty acid flux. *Biochim Biophys Acta Mol Cell Biol Lipids*. 2017;1862(10 Pt B):1146-1154.
19. Zhang X, Xie X, Heckmann BL, et al. Identification of an intrinsic lysophosphatidic acid acyltransferase activity in the lipolytic inhibitor G0/G1 switch gene 2 (G0S2). *FASEB J*. 2019;33(5):6655-6666.
20. Heckmann BL, Zhang X, Xie X, Liu J. The G0/G1 switch gene 2 (G0S2): regulating metabolism and beyond. *Biochim Biophys Acta*. 2013;1831(2):276-281.
21. Kioka H, Kato H, Fujikawa M, et al. Evaluation of intramitochondrial ATP levels identifies G0/G1 switch gene 2 as a positive regulator of oxidative phosphorylation. *Proc Natl Acad Sci U S A*. 2014;111(1):273-278.
22. Lee PH, Yamada T, Park CS, Shen Y, Puppi M, Lacorazza HD. G0S2 modulates homeostatic proliferation of naive CD8(+) T cells and inhibits oxidative phosphorylation in mitochondria. *Immunol Cell Biol*. 2015;93(7):605-615.
23. Kitareewan S, Blumen S, Sekula D, et al. G0S2 is an all-trans-retinoic acid target gene. *Int J Oncol*. 2008;33(2):397-404.
24. Ma T, Dong JP, Sekula DJ, et al. Repression of exogenous gene expression by the retinoic acid target gene G0S2. *Int J Oncol*. 2013;42(5):1743-1753.
25. Khorashad JS, Anand M, Marin D, et al. The presence of a BCR-ABL mutant allele in CML does not always explain clinical resistance to imatinib. *Leukemia*. 2006;20(4):658-663.
26. Cheng Z, Gong Y, Ma Y, et al. Inhibition of BET bromodomain targets genetically diverse glioblastoma. *Clin Cancer Res*. 2013;19(7):1748-1759.
27. Zabriskie MS, Eide CA, Tantravahi SK, et al. BCR-ABL1 compound mutations combining key kinase domain positions confer clinical resistance to ponatinib in Ph chromosome-positive leukemia. *Cancer Cell*. 2014;26(3):428-442.
28. Zhang X, Ren R. Bcr-Abl efficiently induces a myeloproliferative disease and production of excess interleukin-3 and granulocyte-macrophage colony-stimulating factor in mice: a novel model for chronic myelogenous leukemia. *Blood*. 1998;92(10):3829-3840.
29. Kinstrie R, Karamitros D, Goardon N, et al. Heterogeneous leukemia stem cells in myeloid blast phase chronic myeloid leukemia. *Blood Adv*. 2016;1(3):160-169.
30. Varley KE, Mitra RD. Bisulfite patch PCR enables multiplexed sequencing of promoter methylation across cancer samples. *Genome Res*. 2010;20(9):1279-1287.
31. Krueger F, Andrews SR. Bismark: a flexible aligner and methylation caller for bisulfite-seq applications. *Bioinformatics*. 2011;27(11):1571-1572.
32. Ma T, Lopez-Aguilar AG, Li A, et al. Mice lacking G0S2 are lean and cold-tolerant. *Cancer Biol Ther*. 2014;15(5):643-650.
33. Barnes EJ, Eide CA, Kaempf A, et al. Secondary fusion proteins as a mechanism of BCR::ABL1 kinase-independent resistance in chronic myeloid leukaemia. *Br J Haematol*. 2022. <https://doi.org/10.1111/bjh.18515>
34. Marx A, Backes C, Meese E, Lenhof HP, Keller A. EDISON-WMW: exact dynamic programming solution of the Wilcoxon-Mann-Whitney test. *Genom Proteom Bioinform*. 2016;14(1):55-61.
35. Zhao H, Pomicter AD, Eiring AM, et al. MS4A3 promotes differentiation in chronic myeloid leukemia by enhancing common beta-chain cytokine receptor endocytosis. *Blood*. 2022;139(5):761-778.
36. Zheng C, Li L, Haak M, et al. Gene expression profiling of CD34+ cells identifies a molecular signature of chronic myeloid leukemia blast crisis. *Leukemia*. 2006;20(6):1028-1034.
37. Diaz-Blanco E, Bruns I, Neumann F, et al. Molecular signature of CD34(+) hematopoietic stem and progenitor cells of patients with CML in chronic phase. *Leukemia*. 2007;21(3):494-504.
38. Neumann F, Teutsch N, Kliszewski S, et al. Gene expression profiling of Philadelphia chromosome (Ph)-negative CD34+ hematopoietic stem and progenitor cells of patients with Ph-positive CML in major molecular remission during therapy with imatinib. *Leukemia*. 2005;19(3):458-460.
39. Bruennert D, Czibere A, Bruns I, et al. Early in vivo changes of the transcriptome in Philadelphia chromosome-positive CD34+ cells from patients with chronic myelogenous leukaemia following imatinib therapy. *Leukemia*. 2009;23(5):983-985.
40. Tokumaru Y, Yamashita K, Osada M, et al. Inverse correlation between cyclin A1 hypermethylation and p53 mutation in head and neck cancer identified by reversal of epigenetic silencing. *Cancer Res*. 2004;64(17):5982-5987.
41. Kusakabe M, Watanabe K, Emoto N, et al. Impact of DNA demethylation of the G0S2 gene on the transcription of G0S2 in squamous lung cancer cell lines with or without nuclear receptor agonists. *Biochem Biophys Res Commun*. 2009;390(4):1283-1287.
42. Kusakabe M, Kutomi T, Watanabe K, et al. Identification of G0S2 as a gene frequently methylated in squamous lung cancer by combination of in silico and experimental approaches. *Int J Cancer*. 2010;126(8):1895-1902.
43. Yamada T, Park CS, Shen Y, Rabin KR, Lacorazza HD. G0S2 inhibits the proliferation of K562 cells by interacting with nucleolin in the cytosol. *Leuk Res*. 2014;38(2):210-217.
44. Casciano JC, Perry C, Cohen-Nowak AJ, et al. MYC regulates fatty acid metabolism through a multigenic program in claudin-low triple negative breast cancer. *Br J Cancer*. 2020;122(6):868-884.
45. Stine ZE, Walton ZE, Altman BJ, Hsieh AL, Dang CV. MYC, metabolism, and cancer. *Cancer Discov*. 2015;5(10):1024-1039.
46. Notari M, Neviani P, Santhanam R, et al. A MAPK/HNRPK pathway controls BCR/ABL oncogenic potential by regulating MYC mRNA translation. *Blood*. 2006;107(6):2507-2516.
47. Abraham SA, Hopcroft LE, Carrick E, et al. Dual targeting of p53 and c-MYC selectively eliminates leukaemic stem cells. *Nature*. 2016;534(7607):341-346.
48. Eiring AM, Page BD, Kraft IL, et al. Combined STAT3 and BCR-ABL1 inhibition induces synthetic lethality in therapy-resistant chronic myeloid leukemia. *Leukemia*. 2015;29(3):586-597.
49. Herkert B, Eilers M. Transcriptional repression: the dark side of myc. *Genes Cancer*. 2010;1(6):580-586.

50. Cortez D, Reuther G, Pendergast AM. The Bcr-Abl tyrosine kinase activates mitogenic signaling pathways and stimulates G1-to-S phase transition in hematopoietic cells. *Oncogene*. 1997;15(19):2333-2342.
51. Gishizky ML, Witte ON. BCR/ABL enhances growth of multipotent progenitor cells but does not block their differentiation potential in vitro. *Curr Top Microbiol Immunol*. 1992;182:65-72.
52. Russell L, Forsdyke DR. A human putative lymphocyte G0/G1 switch gene containing a CpG-rich island encodes a small basic protein with the potential to be phosphorylated. *DNA Cell Biol*. 1991;10(8):581-591.
53. Cristillo AD, Heximer SP, Russell L, Forsdyke DR. Cyclosporin A inhibits early mRNA expression of G0/G1 switch gene 2 (GOS2) in cultured human blood mononuclear cells. *DNA Cell Biol*. 1997;16(12):1449-1458.
54. Di Tullio A, Vu Manh TP, Schubert A, Castellano G, Månsson R, Graf T. CCAAT/enhancer binding protein alpha (C/EBP(alpha))-induced transdifferentiation of pre-B cells into macrophages involves no overt retrodifferentiation. *Proc Natl Acad Sci U S A*. 2011;108(41):17016-17021.
55. Chambers SM, Boles NC, Lin KY, et al. Hematopoietic fingerprints: an expression database of stem cells and their progeny. *Cell Stem Cell*. 2007;1(5):578-591.
56. Berg JS, Lin KK, Sonnet C, et al. Imprinted genes that regulate early mammalian growth are coexpressed in somatic stem cells. *PLoS One*. 2011;6(10):e26410.
57. Majeti R, Becker MW, Tian Q, et al. Dysregulated gene expression networks in human acute myelogenous leukemia stem cells. *Proc Natl Acad Sci U S A*. 2009;106(9):3396-3401.
58. Andersson A, Edén P, Olofsson T, Fioretos T. Gene expression signatures in childhood acute leukemias are largely unique and distinct from those of normal tissues and other malignancies. *BMC Med Gen*. 2010;3:6.
59. Hu X, Chung AY, Wu I, et al. Integrated regulation of Toll-like receptor responses by Notch and interferon-gamma pathways. *Immunity*. 2008;29(5):691-703.
60. Wildenberg ME, van Helden-Meeuwssen CG, van de Merwe JP, Drexhage HA, Versnel MA. Systemic increase in type I interferon activity in Sjögren's syndrome: a putative role for plasmacytoid dendritic cells. *Eur J Immunol*. 2008;38(7):2024-2033.
61. Novershtern N, Subramanian A, Lawton LN, et al. Densely interconnected transcriptional circuits control cell states in human hematopoiesis. *Cell*. 2011;144(2):296-309.
62. Abrahamsson AE, Geron I, Gotlib J, et al. Glycogen synthase kinase 3beta missplicing contributes to leukemia stem cell generation. *Proc Natl Acad Sci U S A*. 2009;106(10):3925-3929.
63. Perrotti D, Cesi V, Trotta R, et al. BCR-ABL suppresses C/EBPalpha expression through inhibitory action of hnRNP E2. *Nat Genet*. 2002;30(1):48-58.
64. Eiring AM, Harb JG, Neviani P, et al. miR-328 functions as an RNA decoy to modulate hnRNP E2 regulation of mRNA translation in leukemic blasts. *Cell*. 2010;140(5):652-665.
65. Pietarinen PO, Eide CA, Ayuda-Durán P, et al. Differentiation status of primary chronic myeloid leukemia cells affects sensitivity to BCR-ABL1 inhibitors. *Oncotarget*. 2017;8(14):22606-22615.
66. Gianni M, Goracci L, Schlaefli A, et al. Role of cardiolipins, mitochondria, and autophagy in the differentiation process activated by all-trans retinoic acid in acute promyelocytic leukemia. *Cell Death Dis*. 2022;13(1):30.
67. Zagani R, El-Assaad W, Gamache I, Teodoro JG. Inhibition of adipose triglyceride lipase (ATGL) by the putative tumor suppressor GOS2 or a small molecule inhibitor attenuates the growth of cancer cells. *Oncotarget*. 2015;6(29):28282-28295.
68. Edwards M, Mohiuddin SS. *Biochemistry, Lipolysis*. Treasure Island, FL, USA: StatPearls Publishing LLC; 2022.
69. Johnson JL, Johnson LA. Homeostasis of lipid metabolism in disorders of the brain. In: Della Sala S, ed. *Encyclopedia of Behavioral Neuroscience*. 2nd ed. Academic Press; 2021: 372-382.
70. Ciftciler R, Haznedaroglu IC. Tailored tyrosine kinase inhibitor (TKI) treatment of chronic myeloid leukemia (CML) based on current evidence. *Eur Rev Med Pharmacol Sci*. 2021;25(24):7787-7798.
71. Guerzoni C, Bardini M, Mariani SA, et al. Inducible activation of CEBPB, a gene negatively regulated by BCR/ABL, inhibits proliferation and promotes differentiation of BCR/ABL-expressing cells. *Blood*. 2006;107(10):4080-4089.
72. Yokota A, Hirai H, Sato R, et al. C/EBPβ is a critical mediator of IFN-α-induced exhaustion of chronic myeloid leukemia stem cells. *Blood Adv*. 2019;3(3):476-488.
73. Prost S, Relouzat F, Spentchian M, et al. Erosion of the chronic myeloid leukaemia stem cell pool by PPARγ agonists. *Nature*. 2015;525(7569):380-383.
74. Apsel Winger B, Shah NP. PPARγ: welcoming the new kid on the CML stem cell block. *Cancer Cell*. 2015;28(4):409-411.
75. Zandbergen F, Mandard S, Escher P, et al. The G0/G1 switch gene 2 is a novel PPAR target gene. *Biochem J*. 2005;392(Pt 2):313-324.
76. Bonzheim I, Irmeler M, Klier-Richter M, et al. Identification of C/EBPβ target genes in ALK+ anaplastic large cell lymphoma (ALCL) by gene expression profiling and chromatin immunoprecipitation. *PLoS One*. 2013;8(5):e64544.
77. Zhao NQ, Li XY, Wang L, et al. Palmitate induces fat accumulation by activating C/EBPβ-mediated GOS2 expression in HepG2 cells. *World J Gastroenterol*. 2017;23(43):7705-7715.
78. Khan SA, Sathyanarayan A, Mashek MT, Ong KT, Wollaston-Hayden EE, Mashek DG. ATGL-catalyzed lipolysis regulates SIRT1 to control PGC-1alpha/PPAR-alpha signaling. *Diabetes*. 2015;64(2):418-426.
79. Li L, Wang L, Li L, et al. Activation of p53 by SIRT1 inhibition enhances elimination of CML leukemia stem cells in combination with imatinib. *Cancer Cell*. 2012;21(2):266-281.
80. Chen W, Bhatia R. Roles of SIRT1 in leukemogenesis. *Curr Opin Hematol*. 2013;20(4):308-313.
81. Li L, Bhatia R. Role of SIRT1 in the growth and regulation of normal hematopoietic and leukemia stem cells. *Curr Opin Hematol*. 2015;22(4):324-329.
82. Abraham A, Qiu S, Chacko BK, et al. SIRT1 regulates metabolism and leukemogenic potential in CML stem cells. *J Clin Invest*. 2019;129(7):2685-2701.
83. Liu W, Zhu X, Tang L, et al. ACSL1 promotes imatinib-induced chronic myeloid leukemia cell senescence by regulating SIRT1/p53/p21 pathway. *Sci Rep*. 2022;12(1):17990.
84. Naka K. Role of lysophospholipid metabolism in chronic myelogenous leukemia stem cells. *Cancers*. 2021;13(14):3434.
85. Naka K, Ochiai R, Matsubara E, et al. The lysophospholipase D enzyme Gdpd3 is required to maintain chronic myelogenous leukaemia stem cells. *Nat Commun*. 2020;11(1):4681.

86. Jang HJ, Woo YM, Naka K, et al. Statins enhance the molecular response in chronic myeloid leukemia when combined with tyrosine kinase inhibitors. *Cancers*. 2021;13(21):5543.

SUPPORTING INFORMATION

Additional supporting information can be found online in the Supporting Information section at the end of this article.

How to cite this article: Gonzalez MA, Olivas IM, Bencomo-Alvarez AE, et al. Loss of G0/G1 switch gene 2 (G0S2) promotes disease progression and drug resistance in chronic myeloid leukaemia (CML) by disrupting glycerophospholipid metabolism. *Clin Transl Med*. 2022;12:e1146. <https://doi.org/10.1002/ctm2.1146>